Modelling and Control of an Inverted Pendulum Turbine

Sergi Rotger Griful

Kongens Lyngby 2012
IMM-M.Sc.-2012-66

Technical University of Denmark
Informatics and Mathematical Modelling
Building 321, DK-2800 Kongens Lyngby, Denmark
Phone +45 45253351, Fax +45 45882673
reception@imm.dtu.dk
www.imm.dtu.dk IMM-M.Sc.-2012-66

Summary

The current energy situation is untenable in a long term. A change in the energy sector is required and the wind energy is postulated as a good candidate for this evolution.

There are many ways of improving the wind energy, either building bigger structures able to generate large amounts of electricity either investigating new improvements to make wind energy more profitable. In this project the feasibility of a new kind of wind turbine is studied.

This thesis deals with the achievement of getting a proper mathematical model of a new kind of wind turbine, called the inverted pendulum turbine, but also designing a controller able to command this great structure.

The inverted pendulum turbine is inherently unstable system. In order to control this wind turbine an optimal control has been investigated: the linear quadratic regulator.

This project studies the feasibility of this uncommon wind turbine system design but also promotes sustainable energy and opens a wide range of new possible implementations in the world of wind turbines.

Resum

La situació energètica actual és insostenible a llarg termini. El sector energètic està demanant a crits una reestructuració important i l'energia eòlica es postula com possible motor d'aquest canvi.

Hi ha moltes maneres de millorar l'energia eòlica, ja sigui construint aerogeneradors de dimensions més grans capaços de produir més electricitat o investigant noves millores per tal de fer l'energia eòlica més rentable. En aquest projecte s'estudia la viabilitat d'un nou model de turbina vent.

Aquest treball té el repte d'aconseguir un model matemàtic fiable d'aquesta nova turbina de vent, anomenada turbina de pèndul invertit, i dissenyar un regulador capaç de controlar aquesta gran infraestructura.

La turbina de pèndul invertit és, per la seva naturalesa, un sistema inestable. Per tal de poder controlar-la s'ha utilitzat una tècnica de regulació òptima com ara és el control lineal quadràtic.

Aquest projecte estudia la viabilitat d'aquest estrambòtic aerogenerador així com també promou les energies renovables obrint un ampli ventall de futures aplicacions en el món de l'energia eòlica.

Preface

The project was carried out at the department of Informatics and Mathematical Modelling at the Technical University of Denmark with the cooperation of the Danish wind company Vestas Wind Systems A/S in fulfilment of the requirements for acquiring an M.Sc. degree in Industrial Engineering in Automation and Control.

This project was proposed by the engineer Keld Hammerum from Vestas Wind Systems A/S and have been supervised by the control engineer Fabio Caponetti from Vestas Turbines R&D, by the PhD student Mahmood Mirzaei from DTU Informatics, by the Associate Professor Hans Henrik Niemann from DTU Electrical Engineering and by the Associate Professor Niels Kjølstad Poulsen from DTU Informatics.

The thesis deals with the achievement of modelling and controlling a new kind of wind turbine known as the inverted pendulum turbine. The inverted pendulum turbine is a Horizontal Axes Wind Turbine with and additional degree of freedom: the inclination of the tower. The controller then has the goal of maximizing the produced electrical power while avoiding the turbine to collapse.

Lyngby, 16-July-2012

Sergi Rotger Griful

Acknowledgements

As an Erasmus student I had to choose a project to work on before arriving to Denmark. After searching and considering many different options I contacted with the Associate Professor Niels Kjølastad Poulsen who offered me a very interesting and challenging project. For giving me the chance to work with him and for all his support and guidance during the realization of this thesis I would like to express my most sincere gratitude to him.

I would also like to thank the Associate Professor Hans Henrik Niemann for his advices and inspiration, and the PhD student Mahmood Mirzaei for all the time that has dedicated to me which has been very useful and instructive.

I would like to express my gratitude to the control engineer Fabio Caponetti because besides the distance he has always been there ready to help and give me useful advices. I would also like to thank the M.Sc. student Martin Klauco for many fruitful and inspiring discussions.

And last but not least I would like to express my gratitude to my family and friends, specially my mother Eulàlia, my father Jordi, my sister Carla and my girlfriend Núria, because besides the large distance between us I have never felt alone and I have always received support from them.

Nomenclature

v	m/s	Wind speed
$\dot{v}$	m/s^2	Wind acceleration
v_m	m/s	Mean component of the wind speed model
v_t	m/s	Turbulent component of the wind speed model
P_w	W	Power available in the wind
P_r	W	Power extracted by the rotor
P_e	W	Electrical power
η	$-$	Efficiency of mechanical-electrical conversion
ρ_a	kg/m^3	Air density
g	m/s^2	Gravity constant

A_t	m^2	Swept area by the wind turbine blades
R	m	Rotor radius
C_p	$-$	Power coefficient
C_t	$-$	Thrust coefficient
λ	$-$	Tip speed ratio
ω_r	rad/s	Rotor angular speed
ω_g	rad/s	Generator angular speed
β	deg	Pitch angle
T_r	$N\ m$	Aerodynamic torque
T_g	$N\ m$	Generator torque
F_t	N	Thrust force
N	$-$	Gearbox ratio
K_t	N/m	Tower spring constant
D_t	$N/m\ s$	Tower damping constant
M_t	kg	Mass of the tower, rotor, nacelle and hub
K_t^a	N/rad	Tower angular spring constant
D_t^a	Ns/rad	Tower angular damping constant
M_t^a	Ns^2/rad	Angular equivalence to M_t
f_n	Hz	Natural frequency of the tower Fore-Aft
J_g	$kg\ m^2$	Inertia of the generator
J_r	$kg\ m^2$	Inertia of the rotor
J	$kg\ m^2$	Inertia of the generator and rotor

θ	rad	Angle of inclination of the tower
$\dot{\theta}$	rad/s	Speed of inclination of the tower
$\ddot{\theta}$	rad/s^2	Acceleration of inclination of the tower

n_x	$-$	Number of states
n_y	$-$	Number of outputs
n_u	$-$	Number of inputs
n_d	$-$	Number of disturbances

x	$\in \Re^{n_x}$	State vector
u	$\in \Re^{n_u}$	Input vector
y	$\in \Re^{n_y}$	Output vector
x_{ref}	$\in \Re^{n_x}$	Reference state vector
u_{ref}	$\in \Re^{n_u}$	Reference input vector
y_{ref}	$\in \Re^{n_y}$	Reference output vector

A	$\in \Re^{n_x \times n_x}$	State space system matrix
B	$\in \Re^{n_x \times n_u}$	State space input matrix
C	$\in \Re^{n_y \times n_x}$	State space output matrix
D	$\in \Re^{n_y \times n_u}$	State space direct input-output matrix
E	$\in \Re^{n_x \times 1}$	State space states-wind matrix
d_x	$\in \Re^{n_x}$	Affine state vector
d_y	$\in \Re^{n_y}$	Affine output vector
M_c	$\in \Re^{n_x \times (n_x \times n_u)}$	Controllability matrix
M_o	$\in \Re^{(n_x \times n_y) \times n_x}$	Observability matrix
K	$\in \Re^{n_u \times n_x}$	LQR feedback gain matrix
Q	$\in \Re^{n_x \times n_x}$	LQR variables weight matrix
R	$\in \Re^{n_u \times n_u}$	LQR inputs weight matrix
N	$\in \Re^{n_x \times n_u}$	LQR variables-inputs weight matrix
L	$\in \Re^{n_x \times n_y}$	Kalman filter gain matrix
Q_e	$\in \Re^{n_x \times n_x}$	States covariance matrix
R_e	$\in \Re^{n_y \times n_y}$	Outputs covariance matrix
w_k	$\in \Re^{n_x}$	States noise
v_k	$\in \Re^{n_y}$	Measurements noise
d_k	$\in \Re^{n_{d_{in}}}$	Input disturbances
p_k	$\in \Re^{n_{d_{out}}}$	Output disturbances
B_d	$\in \Re^{n_x \times n_{d_{in}}}$	State space input disturbances matrix
C_d	$\in \Re^{n_y \times n_{d_{out}}}$	State space output disturbances matrix

T_s	s	Sampling time
f_s	Hz	Sampling frequency

Contents

Chapter 1

Introduction

According to the *International Energy Agency* (IEA) more than 50% of the final energy consumed in 2009 came from burning oil and gas. This kind of energy sources are contributing with their high CO_2 emissions to the global warming. The energy sources used nowadays and the fact that every day the energy consumption is growing are bringing the world to a dead-end.

To try to redirect the current situation there are two possible solutions: changing the habits of people by trying to reduce the energy consumption and changing the current energy sources by ones with less environment impact like renewable energies.

Changing the habits of people is always a really challenging task and do not seems possible to see results in a short term.

Promoting renewable energies in front of the polluting ones is not easy as well but the energy sector is claiming for a big change.

There are many renewable energies and most of them are growing since the energy change is becoming a necessity. Because of its good results, the wind energy is gaining importance in the energy sector and has experienced a dramatic growth since the turn of the 21st century. According to the *IEA* the global installed capacity at the end of 2011 was around 238 GW, up from 18 GW at

the end of 2000.

Besides the important environmental impact that the wind turbines have to the nature and wildlife they do not have any other big drawbacks. This environmental impact is normally evaluated during the sitting process of wind farms avoiding some places like natural reserves or the main routes of migration birds. Wind turbines are able to generate big amounts of *'clean energy'*, they can readjust the difference between the electrical offer and demand faster than other energy sources... All these facts are making the wind energy a possible way out to the difficult current situation. Companies and governments are aware of this situation and are investing in research and development of wind turbines. A good example of this situation is that, according to the *IEA*, ten European countries have agreed to develop an offshore electricity grid in the North Sea to enable offshore wind developments.

Everyday wind energy companies are fabricating bigger turbines that are able to produce more electrical power. For example the Danish wind turbine developer Edmond Muller has designed a 30 MW wind turbine which is higher than the Eiffel Tower, but no wind company believe in his project. This shows that the size of wind turbine cannot be increased indefinitely, there is definitely an upper limit, there is going to be a moment that increasing the size will not be profitable any more. That is the reason why new technical solutions, such the one developed in this project, are being investigated.

1.1 The Inverted Pendulum Turbine

Current wind turbines are huge structures with an important initial investment. In (Fingersh et al., 2006) there is a large description of the costs of the components of wind turbines and the start-up/installation costs for land based turbines and off-shore turbines. To give an order of magnitude of the costs of a wind turbine in tables 1.1 and 1.2 there is, respectively, a summary of the expenses in the land-based and in the off-shore case.

As it can be seen from the tables 1.1 and 1.2 , the cost of the tower accounts around 10% of the total cost (material and installation) and around 15% of the turbine cost. The large cost of the tower stems from the fact that it needs to be very stiff in order to withstand the bending moments of the thrust force of the wind. One possible solution to reduce the cost of the tower is the inverted pendulum turbine. In figure 1.1 a schematic of this wind turbine is presented.

The inverted pendulum turbine is a new kind of wind turbine which peculiarity

Table 1.1: Land-Based 1.5-MW Baseline Turbine Costs in 2002.(Fingersh et al., 2006)

Component	**Cost [$1.000]**	[%]
Turbine cost	1.036	73.8
Rotor	237	16.9
Drive train, nacelle	617	44.0
Control & Safety	35	2.5
Tower	147	10.4
Station cost	367	26.2
Initial capital cost	1.403	100

Table 1.2: Offshore 3-MW Baseline Turbine Costs in 2005.(Fingersh et al., 2006)

Component	**Cost [$1.000]**	[%]
Turbine cost	2.698	42.2
Rotor	477	7.5
Drive train, nacelle	1.425	22.3
Control & Safety	60	0.9
Tower	415	6.5
Marinization	321	5.0
Station cost	3.331	52.2
Off-shore warranty premium	357	5.6
Initial capital cost	6.386	100

is mounting the tower of the wind turbine in a hinge-like structure. That way the thrust force exerted by the wind could be balanced by the gravitational force of the turbine itself. Then the wind turbine would be free to leans towards the wind and would leave only compression forces to be handled by the tower making it possible to be a lighter and cheaper structure.

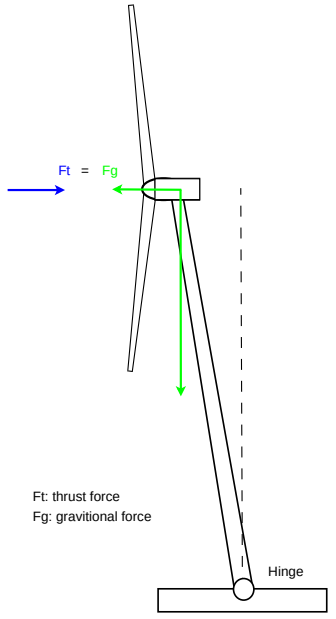

Figure 1.1: The inverted pendulum turbine.

Nowadays the offshore wind energy just can be placed in specific zones with shallow sea ground like Denmark. This is because current offshore wind turbines are stand in the sea ground and if it is very deep the foundation costs are too large to make the initial investment profitable. As it can be seen in table 1.2, the station cost in the offshore wind turbines is more that 50%. A large portion of the cost of the station installation accounts on the foundations and the support structure. With the inverted pendulum turbine this two problems could be solved. The hinge effect in a offshore wind turbine could be obtained by a floating foundation operated by some kind of actuator. That way deep sea ground will not be a problem anymore and the investment of the station installation could be reduced significantly.

A life example of this possible offshore application is found in the *WindFloat project* that the American company Principle Power, Inc. is developing with cooperation with other companies. They have design a floating surface, which would make the hinge effect, and a controller that avoids the tower fore-aft

motion caused by the wind gust an the sea motion. Right now they are still doing test in the coast of Portugal.

1.2 Control

These days wind turbines are controlled by a set of PI(D) controller such the one designed by the *National Renewable Energies Laboratory* in (Jonkman et al., 2009). The performance of this controllers is manually optimized and the tuning process is done by an engineer in an iterative process until the required performance is obtained. Then having good results depend on the experience of the engineer.

A possible alternative to this kind of controllers are the optimal controllers like *Model Predictive Controllers* (MPC) and *Linear Quadratic Regulators* (LQR). This kind of regulators ensure an optimal performance having a good model of the wind turbine. Then the quality of the control action relies on the quality of the model. This is one of the reasons why companies are still working with set of PI(D) instead of optimal controllers.

Today there many techniques of system identification that can get a good models and some control method that are able to minimize the mismatch between a model and its plant. In other sectors like the chemical world MPC has been implemented successfully and its to be expected that in the near future, the PI(D) controllers of the wind turbines would probably be replaced by more efficient controllers such as MPC or LQR. Today there are many studies of this kind of controllers over wind turbines, for example in (Henriksen, 2007) and (Gosk, 2011) the viability of the MPC to control wind turbines is studied and in (Mirzaei et al., 2012b) there is a very interesting approach of the robust MPC of a wind turbine over the full load region.

The Linear Quadratic Regulators are a proven control technique, that compared to the PI(D) ensures optimal performance, but do not need such a large computational models like the MPC. Compared to PI(D) controllers Linear Quadratic Regulators can work over multi-input multi-output (MIMO) systems while PI(D) need to work on single-input single-output(SISO) systems or over a MIMO systems separate in different SISO systems, but that is not always possible. It is important to highlight that wind turbines are MIMO systems and in this project the inverted pendulum turbine has been treated as that. Because of all this reasons the Linear Quadratic Regulator technique has been chosen to control the inverted pendulum turbine.

1.3 Objectives

The main objective of this thesis is to investigate the feasibility of the inverted pendulum turbine. It is expected that the inverted pendulum turbine produces less electricity than other wind turbines because of its hinge tower. The idea is to see how less electricity is produced and how much could the expense of the tower be reduced from a control point of view. Then, with all this data, decide if this project could be profitable or not.

In order to achieve this main goal several sub-objectives need to be accomplish.

First of all a mathematical model of the inverted pendulum turbine has to be obtained. When designing a LQR controller for the wind turbine a model is required.

Once the model of the inverted pendulum turbine is defined the stationary operating points of this turbine need to be identified. To implement a proper control law it is important to identify the steady points. With the model of the system and the steady point one can obtain a linear model.

Finally a controller need to be designed in order to ensure good performance and the stability of the inverted pendulum turbine.

During the fulfilment of this thesis all the objectives mentioned above have been studied deeply.

1.4 Thesis Overview

In the realization of this thesis all the simulations and calculations have been done in *MATLAB*. It is important to highlight that all the simulations have been done in discrete time since that is how controllers work in real applications.

As a reference wind turbine it has been used the 5-MW wind turbine designed by the the *NREL* in (Jonkman et al., 2009) but placing in the bottom of the tower a hinge and considering all the consequences that this implies.

The report of this thesis is organized in four different parts according to chapters:

- **Modelling and Analysis:** In this part a basic introduction to wind energy is done. It is also shown how the model of the inverted pendulum has been obtained. Then an analysis of the control properties of this uncommon wind turbine has been done.
- **Control Methods:** In this part all the theoretical control methods used are introduced.
- **Implementation and Results:** In this part all the methods mentioned in the previous chapter have been put into practice. All the results obtained from the simulations are also shown in this part.
- **Conclusions and Perspectives:** In this final part the conclusions of the project are exposed and the possible future perspective of the thesis are presented.

It is assumed that the reader of this thesis have basic knowledge of physics and control theory. However there is a brief mention of all the important concepts used and a basic introduction to the world of wind energy and wind turbines.

Chapter 2

Modelling and Analysis

In this chapter the reader can find a basic description of wind turbines and wind energy. Then the non-linear model of the inverted pendulum turbine is presented. With the aim of maximizing the produced electrical power and satisfying some restrictions imposed by the wind turbine components the different operation modes of this peculiar wind turbine are defined and the steady state analysis for the baseline wind turbine is done. Finally the linear model is obtained and the basic properties of the system are analysed.

2.1 Wind Turbines and Wind Energy Basics

2.1.1 Wind Energy Conversion Systems

As mentioned in (Sathyajith, 2006) there are many different kind of Wind Energy Conversion Systems (WECS). The most commune *WECS* nowadays are the Horizontal Axis Wind Turbines (HAWT) but it has not always been like this. By the end of the last century there was an intense research on the Vertical Axis Wind Turbines (VAWT) but theses could not be as a reliable alternative as the *HAWT*. In this section a short introduction to the *HAWT* and the different components of this wind turbines is done.

The *HAWT* is the wind turbine that one can see today on places where wind energy is present. They normally have three blades and their tower high can be from some meters up to 100 m. The *HAWT* are big structures composed by many different components, the most important ones are listed below. For a better understanding in figure 2.1 the disposition of all the mentioned components can be seen. All the information has been extracted from (Sathyajith, 2006) and (Friis et al., 2010).

- **Tower** is the part that hold the nacelle (or housing) and the rotor in the desired height. The towers of the HAWT are very stiff in order to withstand the bending moments from the thrust acting, exerted by the wind, on the turbine rotor.
- **Rotor** is the part that receives the energy from the wind and transforms it into mechanical power. The rotor is composed by the blades, the hub, the shaft and other components.
- **Blades** is the part responsible of transforming the kinetic energy from the wind into rotational motion. It is important to know that the blades, in order to control the energy extracted from the wind, are able to pitch. Pitching is the action of the blades of rotating along its axes.
- **Hub** is the part which connects all the blades and contain different components like the pitch system.
- **Main shaft or low speed shaft** is connected with the hub and is responsible of transferring the rotational power into the gear box.
- **Gear box** is the responsible of transforming the low speed rotation coming from the low speed shaft into a more fast rotation which is suitable for the electrical generator.
- **Brake** is the part responsible of stopping the wind turbine, for its safety, when the wind is too fast.
- **High speed shaft** is the part connected between the gear box and the generator.
- **Generator** is the part responsible of the transformation from mechanical power to electrical power.
- **Nacelle or housing** is the part that contains the shafts, gear box, brake and the generator, besides other components.

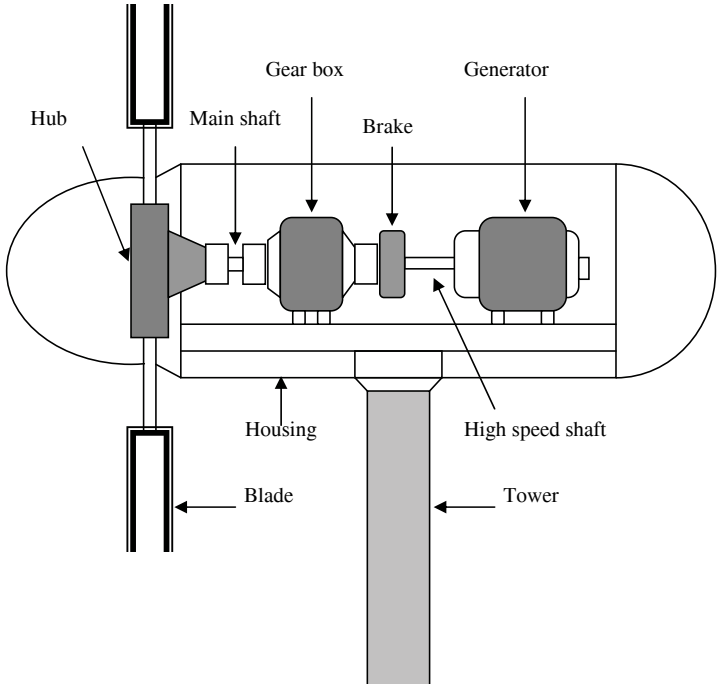

Figure 2.1: Main components of a wind turbine.(Sathyajith, 2006)

2.1.2 Basic Concepts of the Wind Energy Conversion

The information below has been extracted from (Sathyajith, 2006), (Burton et al., 2001) and (Hansen, 2008). The available power of the wind flowing through the circular area swept by the blades of the wind turbine is given by

$$P_w = \frac{1}{2}\rho_a A_t v^3 = \frac{1}{2}\rho_a \pi R^2 v^3 \tag{2.1}$$

where ρ_a is the air density, v is the speed of the wind, A_t is the area of the wind rotor and R is the radius of the rotor disc. There are many factors like temperature, atmospheric pressure, elevation and air constituents that can affect the air density but in this project they are not considered. In appendix B all the data used in this thesis can be found.

It is physically impossible to extract all the available power of the wind, oth-

erwise the wind speed at the rotor front would be zero and the rotation of the rotor would stop. It becomes necessary to introduce the concept of the power coefficient C_p

$$P_r = P_w C_p \tag{2.2}$$

C_p is the ratio between the power extracted by the rotor, P_r, and the power available from the wind, P_w, and it has a theoretical upper limit of $\frac{16}{27}$ known as Betz limit. Modern wind turbines have a maximum power coefficient around 0.5. The C_p coefficient is function of the pitch angle of the blades β and of the *tip speed ratio* λ, which is the ratio between the linear velocity of the tip of the blades and the wind speed

$$\lambda = \frac{\omega_r R}{v} \tag{2.3}$$

The pitch angle is the rotational angle of the blades along their axes. When β is zero the blades are completely perpendicular to the wind. The figure 2.2 helps to understand better the concept of the pitch angle β.

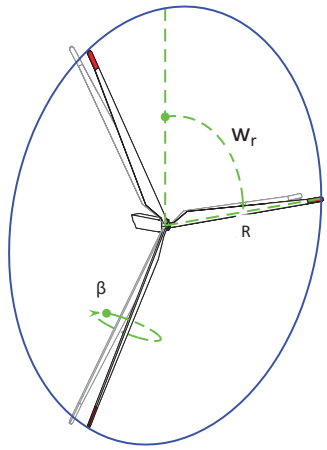

Figure 2.2: Detail of the pitch angle β and the rotational speed w_r.(Henriksen, 2007)

The aerodynamic torque generated by the wind is given by the ratio between P_r and w_r

$$T_r = \frac{1}{\omega_r} P_r = \frac{1}{\omega_r} \frac{1}{2} \rho_a \pi R^2 v^3 C_p \tag{2.4}$$

The thrust force experienced by the rotor as an action of the wind is given by

$$F_t = \frac{1}{2} \rho_a \pi R^2 v^2 C_t \tag{2.5}$$

where C_t is the thrust coefficient and is the ratio between the actual torque developed by the rotor and the theoretical torque. The C_t is also function of the pitch angle β and of the *tip speed ratio* λ.

In figures 2.3 to 2.6 the curves of the power coefficient C_p and torque coefficient C_t of the baseline wind turbine are shown in detail.

To transform the mechanical power extracted from the wind by the rotor, P_r, into electrical power P_e the power goes through many different components(the low speed shaft, the gear box...) that have losses. Taking on account this fact, the electrical power is given by

$$P_e = \eta P_r \tag{2.6}$$

where η is the efficiency factor. Without loss of generality η has been considered equal to 1.

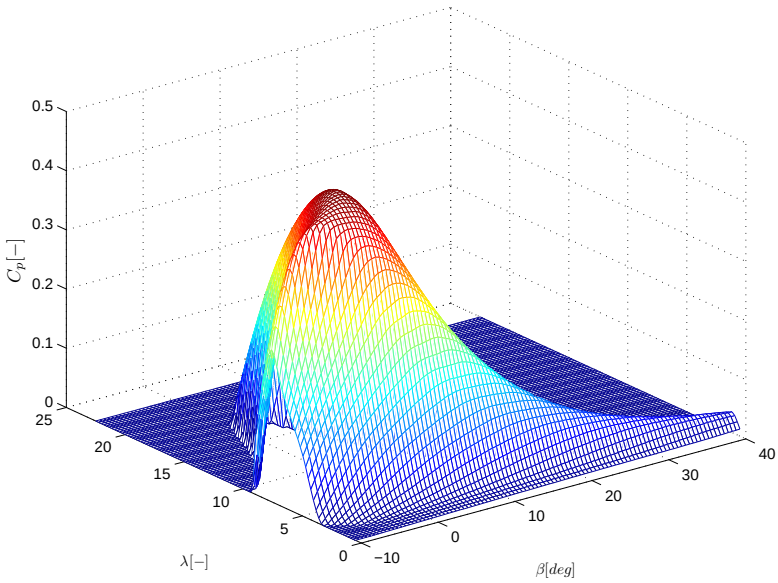

Figure 2.3: Power coefficient C_p [-].

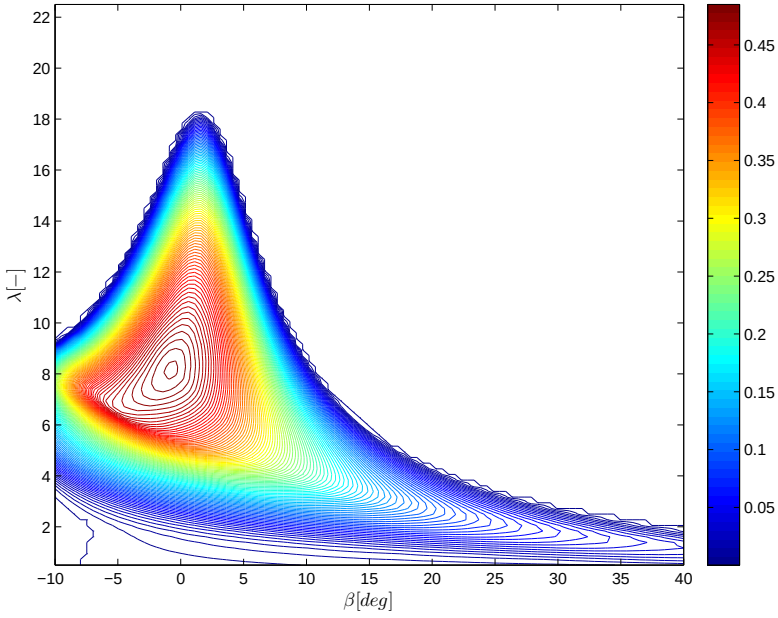

Figure 2.4: Top view of the power coefficient C_p [-].

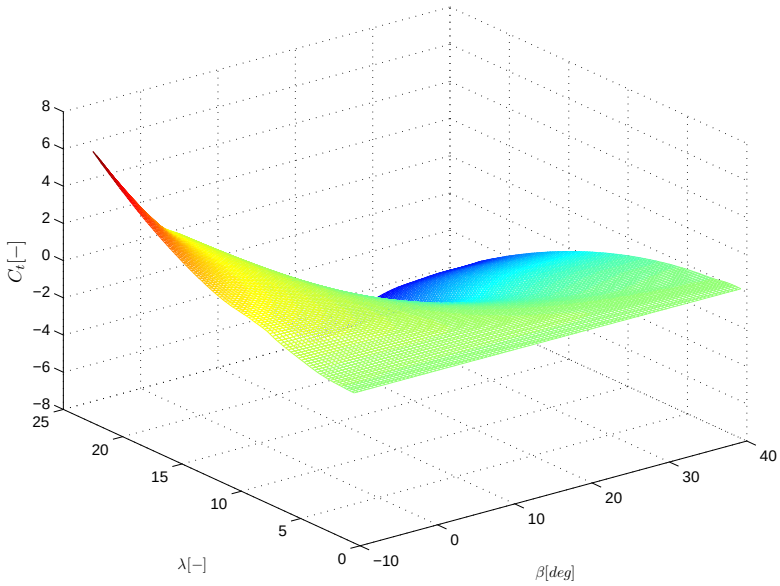

Figure 2.5: Thrust coefficient C_t [-].

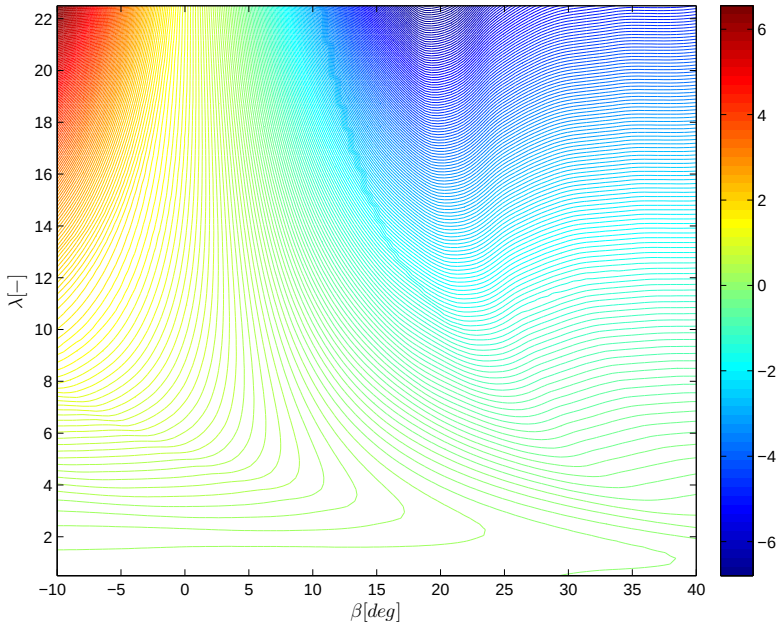

Figure 2.6: Top view of the thrust coefficient C_t [-].

2.2 Non-Linear Model

Wind turbines are huge structures which are composed by many different components. Due to the large number of elements and the complexity of some of them it is not easy to get a precise model of a wind turbine. It is important to know that perfect models do not exist, all that one can do to get a better model is to include additional effects and degrees of freedom.

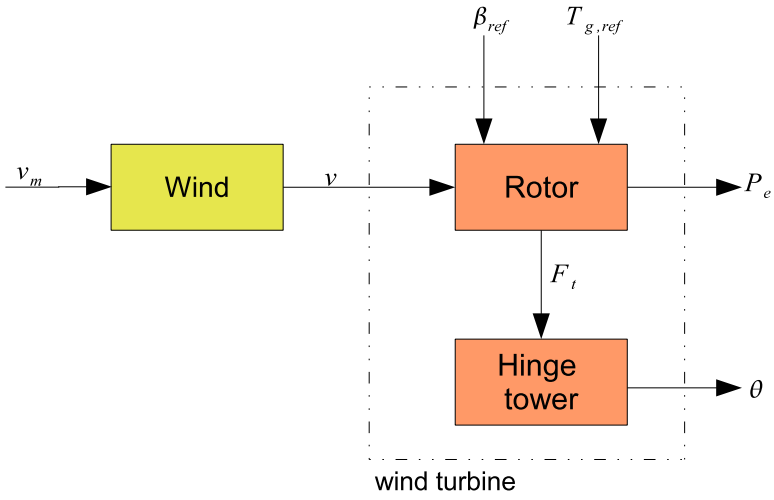

Figure 2.7: Wind turbine and wind model.

In this thesis a model of the inverted pendulum turbine has been obtained. In figure 2.7 there is a bloc diagram of all the parts that are considered in the model. In yellow the stochastic model of the wind that is explained later and in orange the model of the wind turbine. The wind turbine model is composed by two sub-models: the rotor and the hinge tower. These sub-models are explained in detail in the next sections.

2.2.1 Rotor

The model of the rotor is composed by many components and some of them have already been introduced to the reader in section 2.1.1.

The differential equation that models the dynamics of the rotor is

$$J\dot{\omega}_r = \frac{P_r}{\omega_r} - NTg \tag{2.7}$$

This equation expresses the variation of the angular velocity. Using some of the formulas introduced in section 2.1.2 the equation 2.7 can be expressed as

$$J\dot{\omega}_r = Tr - NTg = \frac{1}{\omega_r}\frac{1}{2}\rho_a \pi R^2 v^3 C_p - NT_g \tag{2.8}$$

It can be seen that the rotor dynamical equation is non-linear. Some of the non-linearities are really complex, like the power coefficient C_p shown in figure 2.3.

2.2.2 Hinge Tower

The idea of inverted pendulum turbine has already been introduced in section 1.1 but a summary of the concept is done.

The peculiarity of the inverted pendulum turbine is the tower, which has a hinge in its bottom. That hinge allows the turbine to balance forwards and backwards and reduces the mechanical stress of the tower making it possible to have lighter and cheaper structure.

When modelling the inverted pendulum turbine, the tower has been considered like an inverted pendulum, with a pivot point in the bottom, a rigid stick and all the mass concentrated in the center of mass of the tower. Figure 2.8 helps to understand the simplification made.

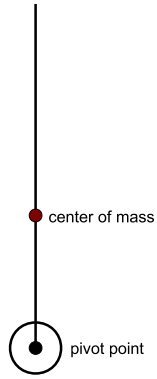

Figure 2.8: Hinge tower simplification.

The force diagram of the hinge tower is like shown in figure 2.9. It is important to notice that the mass of the different components of the wind turbine is separated in two parts: the mass of the tower m_2 and the other masses m_1. The mass of the tower is considered to be centred on the center of mass of the tower h_2 while the mass of the hub, nacelle and rotor is centred on the top of the tower h_1.

If the tower is modelled as a spring-mass-damper system, then the equation that models the dynamics of the hinge tower is

$$h_1(M_t^a\ddot{\theta} + D_t^a\dot{\theta} + K_t^a\theta) = h_1(m_1 g sin\theta - F_t) + h_2 m_2 g sin\theta \tag{2.9}$$

Having a pivot point in the bottom of the tower makes the spring constant zero and the differential equation is

$$h_1(M_t^a\ddot{\theta} + D_t^a\dot{\theta}) = h_1(m_1 g sin\theta - F_t) + h_2 m_2 g sin\theta \tag{2.10}$$

It can be seen that, again, the differential equation that models the dynamics of the hinge tower is non-linear. Notice that, by design, the model does not reflect tower vibration.

As mentioned before the advantage of the inverted pendulum turbine is having a lighter and cheaper structure. In this thesis the mass of the tower has not been reduced. A broad discussion of this simplification can be found below.

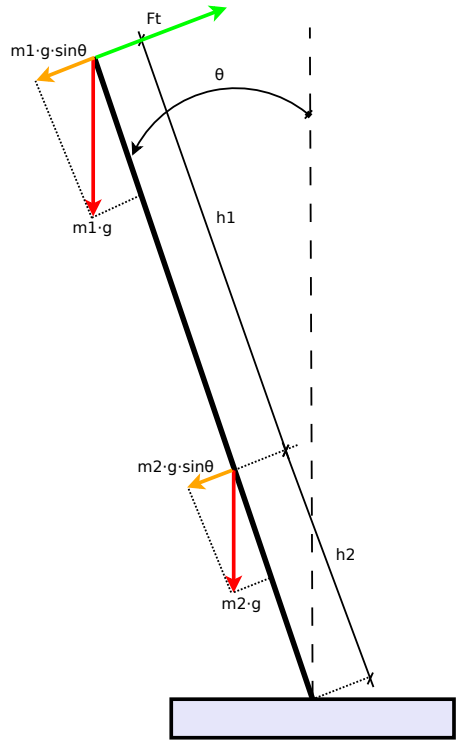

Figure 2.9: Force diagram of the inverted pendulum turbine.

The inclination of the tower can be found from the torque equilibrium equation

$$h_1(F_t - m_1 g sin\theta) - h_2 m_2 g sin\theta = 0 \tag{2.11}$$

Using as a reference the baseline wind turbine from the *NREL* with a hinge in its bottom (in appendix B all the relevant data of this wind turbine is shown) the equation 2.11 has been solved for many different reductions of the mass of the tower. In figure 2.10 all the reductions considered are shown. Notice that the percentage in the figure means how is the new mass compared to the initial

one, so 100% means no mass reduction and 60% means 40% of mass reduction.

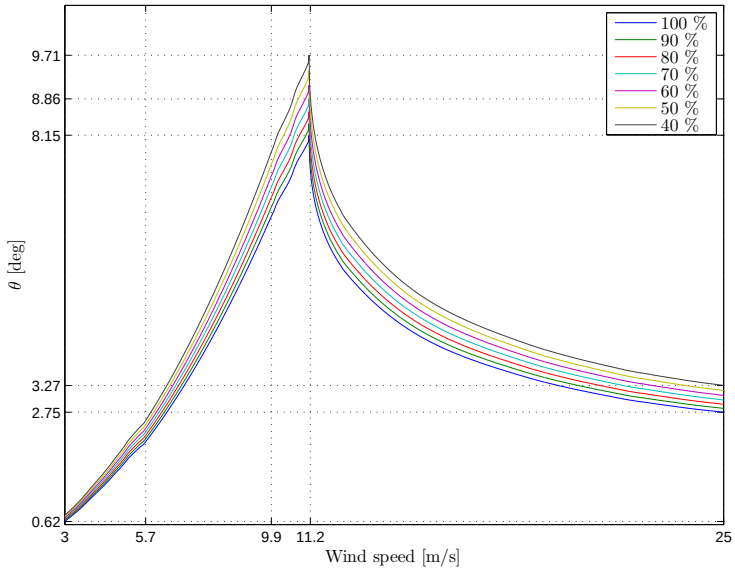

Figure 2.10: Tower inclination for different masses.

It can be seen that if there is no reduction of the mass the maximum inclination of the tower is 8.15 degrees while if the mass of the tower is 40% of the initial value the maximum inclination of the tower is 9.71 degrees. Since the inclination plot is not very different with the initial mass than with the 40% of the initial value no mass reductions has been considered.

2.3 Operation Modes and Steady State Analysis

2.3.1 Operation Regions Definition

Current wind turbines work in a specific wind speed range. The limits of these range are known as *cut-in* and *cut-out speed*. As mentioned in (Burton et al., 2001) the *cut-in speed* is that wind speed at which the turbine starts to generate power and the *cut-out* speed is when the turbine shuts-down to prevent itself to be exposed to extreme loads. The latter might be subject to limitations due to requirements in each country's grid codes.

The main objective of a wind turbines is to maximize the produced electrical power. Notice that in this project the main objective is to avoid the collapse of the tower but maximizing the produced electrical power is also an important objective. So, for each wind speed in the range specified the electrical power is maximized

$$max(P_e) = max(\frac{1}{2}\rho_a \pi R^2 v^3 C_p(\lambda, \beta)) \tag{2.12}$$

subject to

$$0 \leq P_e \leq P_{rated} \tag{2.13}$$

$$\omega_{r_{min}} \leq \omega_r \leq \omega_{r_{rated}} \tag{2.14}$$

These are some physical restrictions imposed by the generator that need to work in between some limits. Notice that, from the equation 2.12, to maximize the power the only parameter that can be controlled is the C_p which depend on the pitch angle β and the tip speed ratio λ. Just as a remind the equation 2.3 is presented again

$$\lambda = \frac{\omega_r R}{v} \tag{2.15}$$

To achieve the goal of maximizing the power and holding the constrains imposed by the generator four regions are defined:

- **Low region (I):** In this region the rotational speed is kept at its lowest value $\omega_{r_{min}}$ while the power produced is maximized. For a given v the λ is also given since the ω_r is constant

$$\lambda_I = \frac{\omega_{r_{min}} R}{v} \tag{2.16}$$

  Then to maximize the power the chosen β has to maximize the C_p. The upper limit of this region is defined by

$$v_1 = \frac{\omega_{r_{min}} R}{\lambda^*} \tag{2.17}$$

  where λ^* is the optimal tip speed ratio defined in the mid region by the equation 2.18.

- **Mid region (II):** In this region the power coefficient C_p is kept at is maximum value, so the β and the λ are the optimal ones

$$(\lambda^*, \beta^*) = max(C_p(\lambda, \beta)) \tag{2.18}$$

  This generates a linear relation between the ω_r and v

$$\omega_r = \frac{\lambda^* v}{R} \tag{2.19}$$

  The upper limit of this region is defined by

$$v_2 = \frac{\omega_{r_{rated}} R}{\lambda^*} \tag{2.20}$$

- **High region (III):** In this region the ω_r is kept at its rated value but not the electrical power. For a given v the λ is defined

$$\lambda_{III} = \frac{\omega_{r_{rated}} R}{v} \tag{2.21}$$

  and the β is decide in order to maximize the electrical power. The upper limit of this region is reached when the produced electrical power achieves its rated value.

- **Top region (IV):** In this region the electrical power is kept at its rated value. For a given v the λ is defined

$$\lambda_{IV} = \frac{\omega_{r_{rated}} R}{v} \tag{2.22}$$

Since there is the restriction that the electrical power cannot exceed the rated value the pitch angle is chosen in a way that the condition below is hold

$$\frac{1}{2}\rho_a \pi R^2 v^3 C_p(\lambda_{IV}, \beta) = P_{rated} \tag{2.23}$$

The upper limit of this region is the *cut-out speed* already defined.

To absorb better all the concepts mentioned above in the table 2.1 there is a summary of the different characteristics for each region. In the next section there are some plots, of the reference wind turbine, that may help to understand better all the regions defined.

2.3.2 Steady State Analysis of the Reference Wind Turbine

The reference wind turbine used in this project is a 5 MW wind turbine designed by *National Renewable Energies Laboratory* (Jonkman et al., 2009) but with a hinge in the bottom of the tower and all the consequence that this implies. In table 2.2 the main characteristics of this wind turbine are shown. For more information about the reference wind turbine a summary of the characteristic can be found in appendix B.

The wind speed that defines the four regions mentioned in the previous section for the reference turbine can be found in table 2.3. Notice that the high region (region III) is narrow.

In figures 2.11 to 2.17 the steady values of the reference wind turbine are shown. It is important to highlight that this steady values are the same as a normal wind turbine, a wind turbine with a stiff tower.

Table 2.1: Region Characteristics.

Region	v interval	ω_r	λ	β
I	(v_{cut-in}, v_1)	$\omega_{r_{min}}$	$\omega_{r_{min}} R \ / \ v$	$\beta = max(C_p(\lambda_I, \beta))$
II	(v_1, v_2)	$\lambda^* v \ / \ R$	λ^*	β^*
III	(v_2, v_3)	$\omega_{r_{rated}}$	$\omega_{r_{rated}} R \ / \ v$	$\beta = max(C_p(\lambda_I II, \beta))$
IV	$(v_3, v_{cut-out})$	$\omega_{r_{rated}}$	$\omega_{r_{rated}} R \ / \ v$	$\beta = P_e = P_{rated}$

Table 2.2: Reference Turbine Basic Characteristics.(Jonkman et al., 2009)

Rated power	5 MW
Configuration	3 blades
Rotor diameter	126 m
Hub heigh	90 m

Table 2.3: Wind Speed Regions for the Reference Turbine.

v_{cut-in}	v_1	v_2	v_3	$v_{cut-out}$
3 m/s	5.6 m/s	9.9 m/s	11.2 m/s	25 m/s

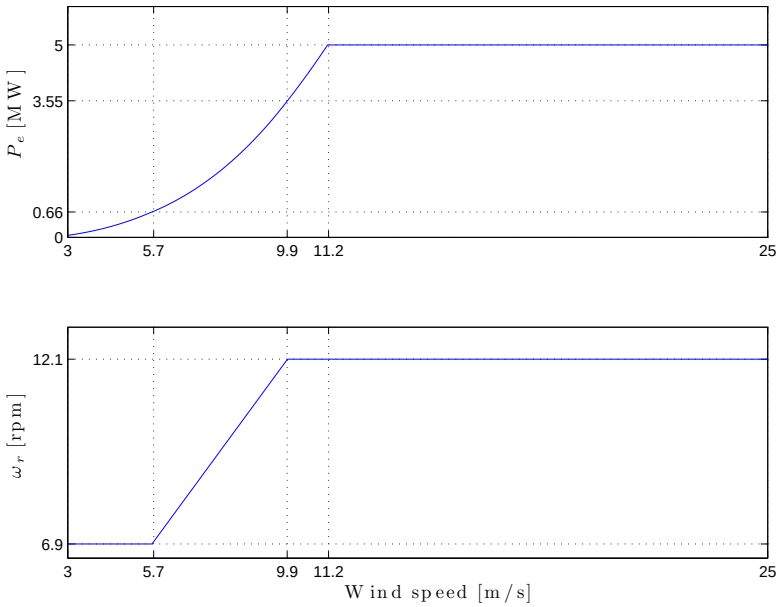

Figure 2.11: Electrical power and rotational speed with respect to the wind.

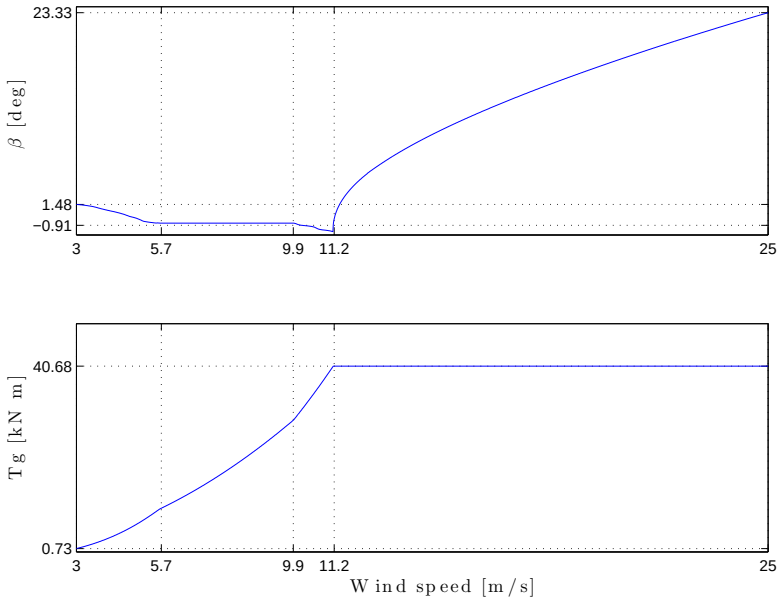

Figure 2.12: Pitch angle and generator torque with respect to the wind.

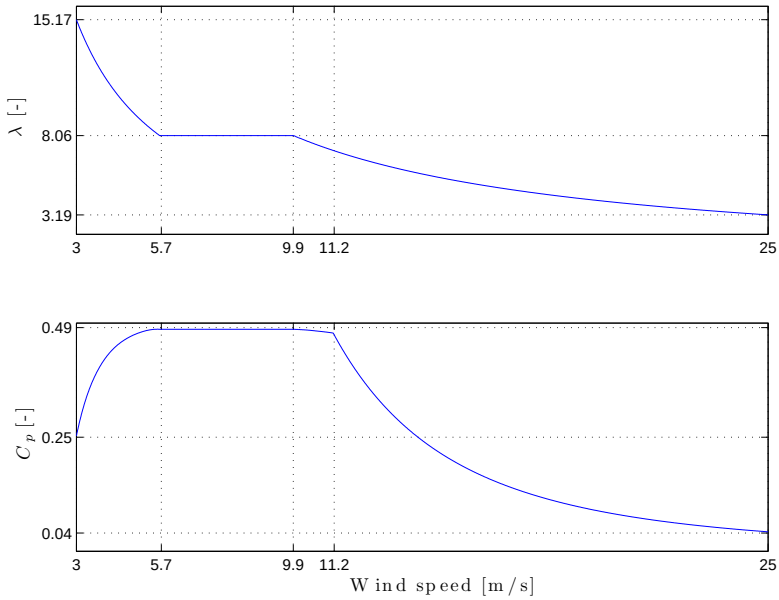

Figure 2.13: Tip speed ratio and power coefficient with respect to the wind.

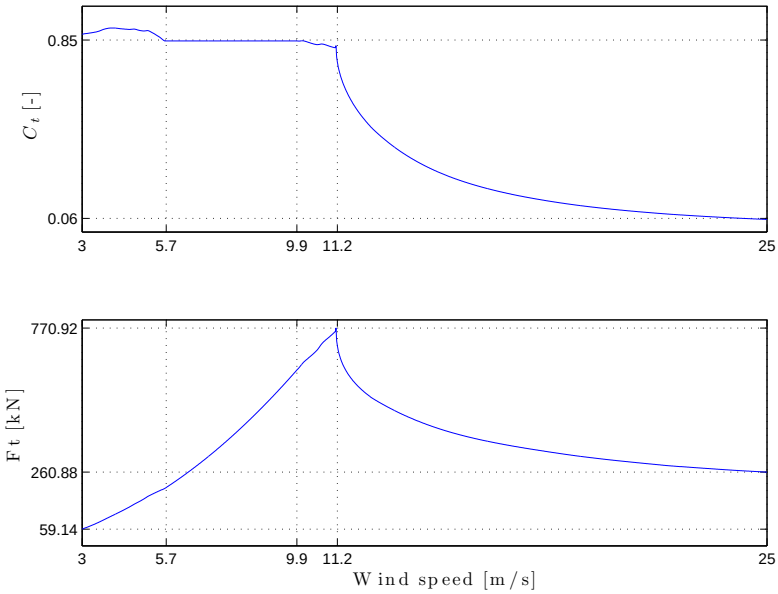

Figure 2.14: Thrust coefficient and thrust force with respect to the wind.

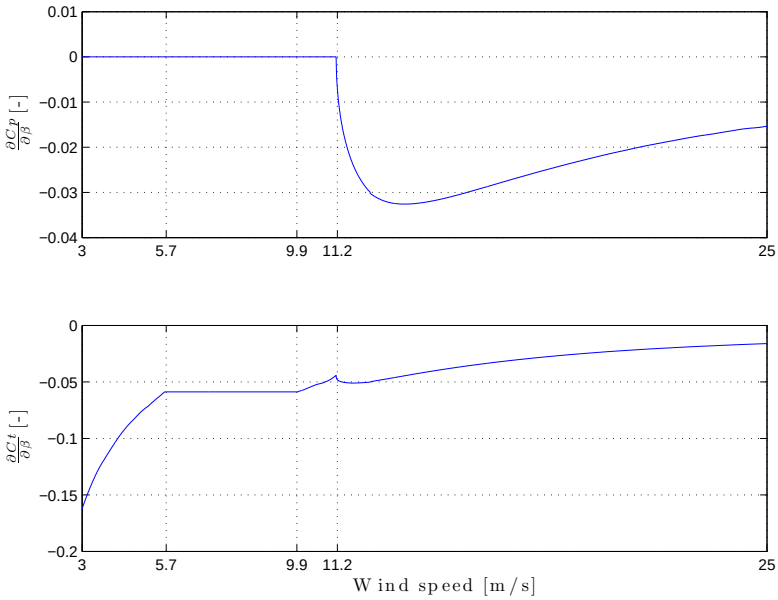

Figure 2.15: Power and thrust coefficient derivatives against pitch with respect to the wind.

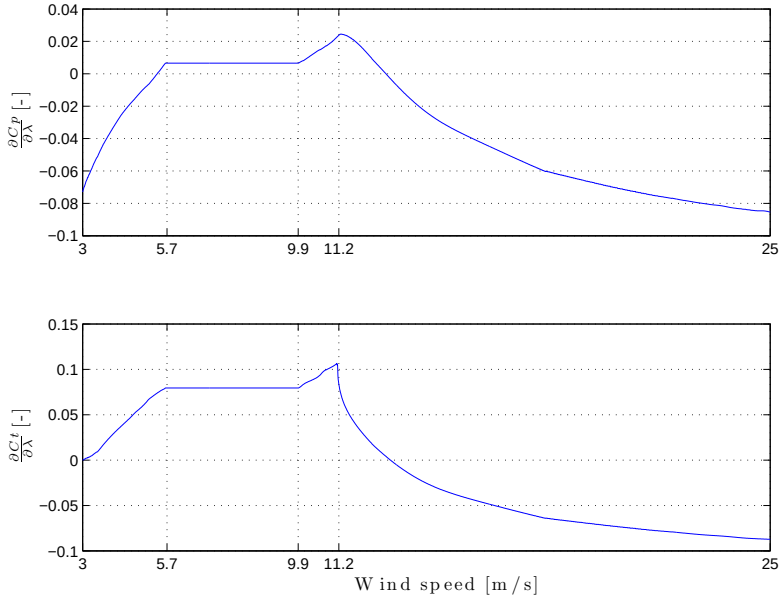

Figure 2.16: Power and thrust coefficient derivatives against tip speed ratio with respect to the wind.

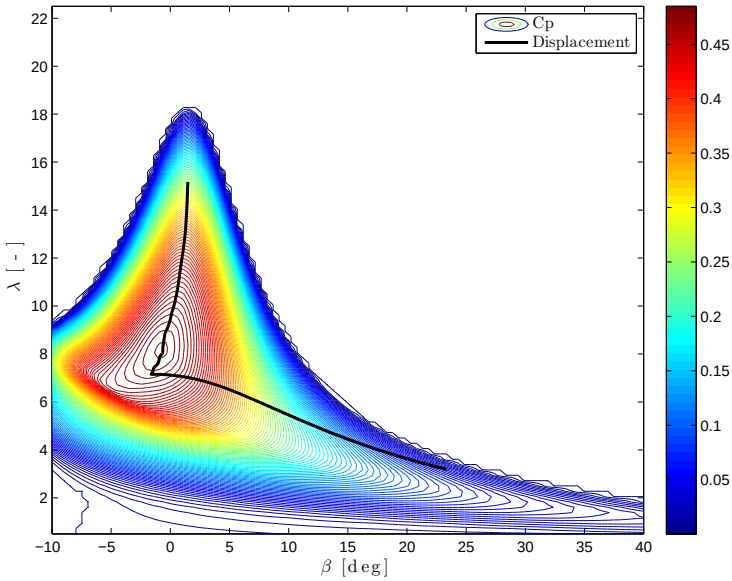

Figure 2.17: Top view of the Cp curve with the reference displacement in black.

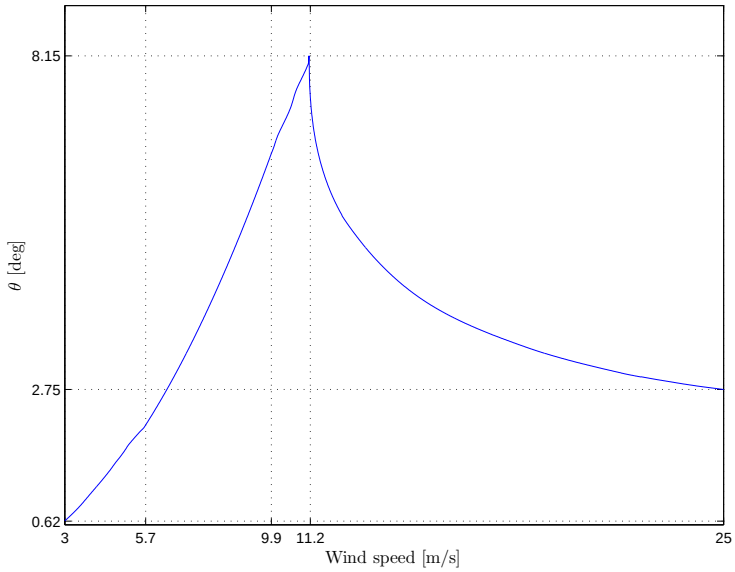

Figure 2.18: Angle of inclination with respect to the wind.

Once the thrust force is known for each wind speed the inclination of the tower can easily be calculated by the torque equilibrium equation

$$h_1(F_t - m_1 g sin\theta) - h_2 m_2 g sin\theta = 0 \tag{2.24}$$

The results of solving the equation 2.24 are shown in figure 2.18. Notice that the steady value of the speed of inclination $\dot{\theta}$ is zero for all the wind speed range since in steady state the tower is not moving.

2.4 Linear Model

In this section the linear model of the inverted pendulum turbine and of the stochastic wind are explained.

2.4.1 Wind Turbine Model

The complete model of the inverted pendulum turbine is a third order system which differential dynamical equations are

$$J\dot{\omega}_r = T_r - NT_g \tag{2.25}$$

$$h_1(M_t^a\ddot{\theta} + D_t^a\dot{\theta}) = h_1(m_1 g sin\theta - F_t) + h_2 m_2 g sin\theta \tag{2.26}$$

Using as a states

$$\mathbf{x} = \begin{bmatrix} \omega_r \\ \theta \\ \dot{\theta} \end{bmatrix} \tag{2.27}$$

as an inputs

$$\mathbf{u} = \begin{bmatrix} \beta \\ T_g \end{bmatrix} \tag{2.28}$$

as a measurements or outputs

$$\mathbf{y} = \begin{bmatrix} P_e \\ \omega_r \\ \theta \end{bmatrix} \tag{2.29}$$

and as a disturbance the wind speed v the non-linear system can be expressed

in state space description as

$$\dot{x} = \begin{bmatrix} \frac{1}{J}[T_r - NTg] \\ \dot{\theta} \\ \frac{h_1(m_1 g sin\theta - F_t) + h_2 m_2 g sin\theta - h_1 D_t^a \dot{\theta}}{h_1 M_t^a} \end{bmatrix} = \begin{bmatrix} f_1(x,u,v) \\ f_2(x,u,v) \\ f_3(x,u,v) \end{bmatrix} \quad (2.30)$$

$$y = \begin{bmatrix} P_e \\ \omega_r \\ \theta \end{bmatrix} = \begin{bmatrix} NT_g\omega_r \\ \omega_r \\ \theta \end{bmatrix} = \begin{bmatrix} g_1(x,u,v) \\ g_2(x,u,v) \\ g_3(x,u,v) \end{bmatrix} \quad (2.31)$$

It is important to highlight that all the considered outputs can be measured with sensors.

Once the non-linear system is expressed in state space and providing all the steady points getting the linearized model is straightforward

$$\Delta\dot{x} = A\Delta x + B\Delta u + E\Delta v \quad (2.32)$$
$$\Delta y = C\Delta x + D\Delta u \quad (2.33)$$

where the matrices are

$$A = \begin{bmatrix} \frac{\partial f_1}{\partial \omega_r} & \frac{\partial f_1}{\partial \theta} & \frac{\partial f_1}{\partial \dot{\theta}} \\ \frac{\partial f_2}{\partial \omega_r} & \frac{\partial f_2}{\partial \theta} & \frac{\partial f_2}{\partial \dot{\theta}} \\ \frac{\partial f_3}{\partial \omega_r} & \frac{\partial f_3}{\partial \theta} & \frac{\partial f_3}{\partial \dot{\theta}} \end{bmatrix}_{(x^*,u^*,v^*)} \quad B = \begin{bmatrix} \frac{\partial f_1}{\partial \beta} & \frac{\partial f_1}{\partial T_g} \\ \frac{\partial f_2}{\partial \beta} & \frac{\partial f_2}{\partial T_g} \\ \frac{\partial f_3}{\partial \beta} & \frac{\partial f_3}{\partial T_g} \end{bmatrix}_{(x^*,u^*,v^*)} \quad (2.34)$$

$$C = \begin{bmatrix} \frac{\partial g_1}{\partial \omega_r} & \frac{\partial g_1}{\partial \theta} & \frac{\partial g_1}{\partial \dot{\theta}} \\ \frac{\partial g_2}{\partial \omega_r} & \frac{\partial g_2}{\partial \theta} & \frac{\partial g_2}{\partial \dot{\theta}} \\ \frac{\partial g_3}{\partial \omega_r} & \frac{\partial g_3}{\partial \theta} & \frac{\partial g_3}{\partial \dot{\theta}} \end{bmatrix}_{(x^*,u^*,v^*)} \quad D = \begin{bmatrix} \frac{\partial g_1}{\partial \beta} & \frac{\partial g_1}{\partial T_g} \\ \frac{\partial g_2}{\partial \beta} & \frac{\partial g_2}{\partial T_g} \\ \frac{\partial g_3}{\partial \beta} & \frac{\partial g_3}{\partial T_g} \end{bmatrix}_{(x^*,u^*,v^*)} \quad (2.35)$$

$$E = \begin{bmatrix} \frac{\partial f_1}{\partial v} \\ \frac{\partial f_2}{\partial v} \\ \frac{\partial f_3}{\partial v} \end{bmatrix}_{(x^*,u^*,v^*)} \quad (2.36)$$

and vectors are

$$\Delta\dot{x} = \dot{x} - x^* \qquad \Delta x = x - x^* \qquad \Delta u = u - u^* \tag{2.37}$$

$$\Delta v = v - v^* \qquad \Delta y = y - y^* \tag{2.38}$$

Notice that all the matrices are evaluated in the steady points. In the previous section it is deduced that the steady points depend on the wind speed: per each wind speed there is a set of steady points. Then, as the linear model depend on the steady points, per each wind speed there is a different linear model. From now on and for a matter of commodity the evaluation of the matrices on the steady points will be omitted.

Calculating all the derivatives the matrices obtained are

$$A = \begin{bmatrix} a_{11} & 0 & 0 \\ 0 & 0 & 1 \\ a_{31} & a_{32} & a_{33} \end{bmatrix} \tag{2.39}$$

where

$$a_{11} = \frac{\rho_a \pi R^2 v^3}{2J\omega_r^2}[\frac{\omega_r R}{v}\frac{\partial C_p(\lambda,\beta)}{\partial\lambda} - C_p(\lambda,\beta)] \qquad a_{33} = \frac{-D_t^a}{M_t^a} \tag{2.40}$$

$$a_{31} = \frac{-\rho_a R^2 \pi v^2}{2M_t^a}\frac{R}{v}\frac{\partial C_t(\lambda,\beta)}{\partial\lambda} \qquad a_{32} = \frac{h_1 m_1 g cos\theta + h_2 m_2 g cos\theta}{h_1 M_t^a} \tag{2.41}$$

$$B = \begin{bmatrix} \frac{\rho_a \pi R^2 v^3}{2J\omega_r}\frac{\partial C_p(\lambda,\beta)}{\partial\beta} & \frac{-N}{J} \\ 0 & 0 \\ \frac{-\rho_a R^2 \pi v^2}{2M_t^a}\frac{\partial C_t(\lambda,\beta)}{\partial\beta} & 0 \end{bmatrix} \tag{2.42}$$

$$C = \begin{bmatrix} NT_g & 0 & 0 \\ 1 & 0 & 0 \\ 0 & 1 & 0 \end{bmatrix} \qquad D = \begin{bmatrix} 0 & N\omega_r \\ 0 & 0 \\ 0 & 0 \end{bmatrix} \tag{2.43}$$

$$E = \begin{bmatrix} \frac{\rho_a \pi R^2}{2J\omega_r}[3v^2 C_p(\lambda,\beta) - vR\omega_r \frac{\partial C_p(\lambda,\beta)}{\partial \lambda}] \\ 0 \\ \frac{-\rho_a \pi R^2}{M_t^a}[2vC_t(\lambda,\beta) - \omega_r R \frac{\partial C_t(\lambda,\beta)}{\partial \lambda}] \end{bmatrix} \tag{2.44}$$

2.4.2 The Wind Model

The variations of the wind speed can be caused by many different factors. One of these factors is the geographical position: the wind speed can be very different depending on the zones, for example, the wind speed in zones close to the water is normally higher than inland. In (Burton et al., 2001) there is an extended explanation of some factors that affect the wind speed. In this thesis all these variations of the wind speed will not be considered.

It is important to remark that in this project the yaw rotation of the turbine is not considered since the time constant of the change of the wind direction is, as mentioned in (Henriksen, 2007), about quarters of hours or hours, which is slowly compared to the variations considered in this thesis.

The wind can be modelled as a very complex system, depending on how many factors are considered. In this thesis the wind is approximated as a second order system like in (Xin et al., 1997) and (Gosk, 2011). In the model used there are two components of the wind:

- v_m: a slowly varying wind speed.
- v_t: a fast varying turbulent component.

The wind model is

$$v = v_m + v_t \tag{2.45}$$

where

$$v_t = \frac{k}{(p_1 s + 1)(p_2 s + 1)} e \tag{2.46}$$

$$e \in N(0,1) \tag{2.47}$$

with k, p_1 and p_2 are functions of v_m. In figure 2.19 the characteristic of the wind model can be seen.

The turbulent wind model can be formulated as a state space description.

$$\begin{bmatrix} \dot{v}_t \\ \ddot{v}_t \end{bmatrix} = \begin{bmatrix} 0 & 1 \\ \frac{-1}{p_1 p_2} & \frac{-p_1 - p_2}{p_1 p_2} \end{bmatrix} \begin{bmatrix} v_t \\ \dot{v}_t \end{bmatrix} + \begin{bmatrix} 0 \\ \frac{k}{p_1 p_2} \end{bmatrix} e \tag{2.48}$$

$$e \in N(0,1) \tag{2.49}$$

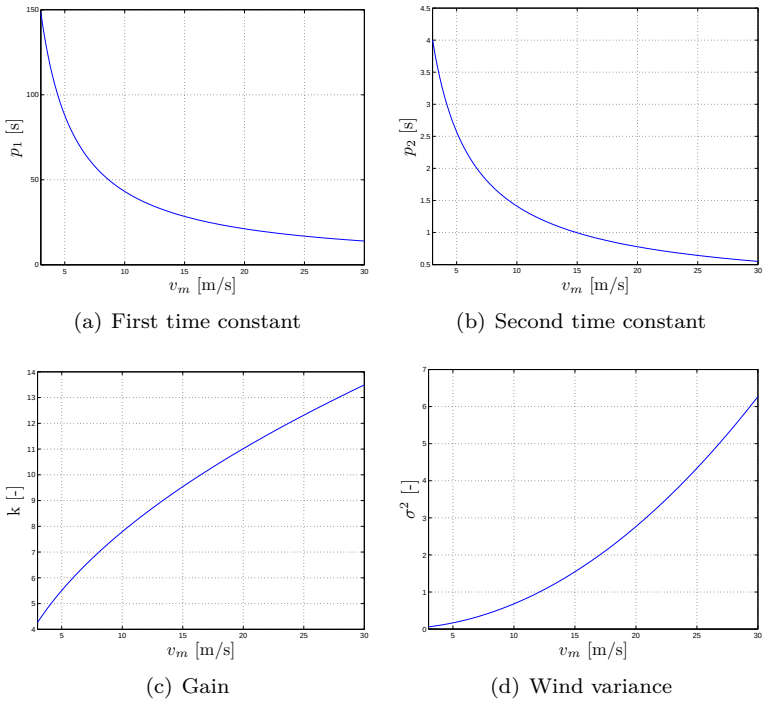

(a) First time constant

(b) Second time constant

(c) Gain

(d) Wind variance

Figure 2.19: Properties of the stochastic wind depending on v_m.

An illustrative example of the result of using this stochastic model for the wind is shown in figure 2.20. It can be seen that for a bigger mean wind speed v_m the

variation of the wind increases as shown in figure 2.19. This difference between variances can be appreciated because both wind data have been generated with the same random numbers.

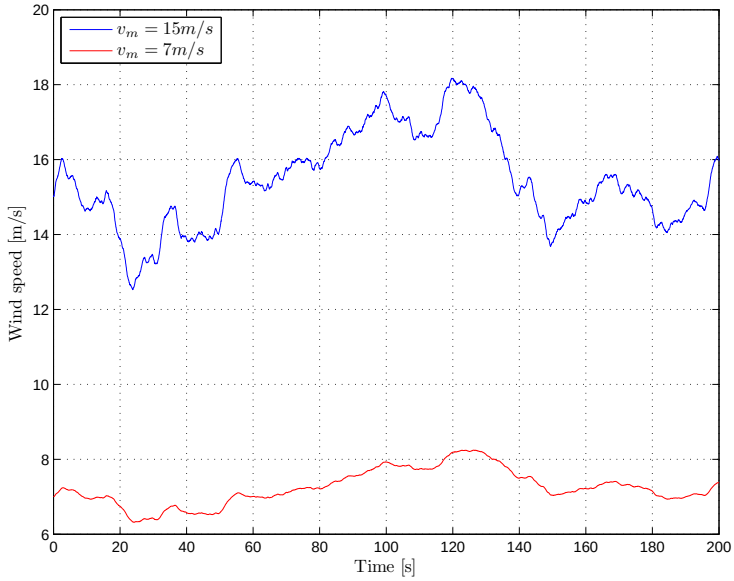

Figure 2.20: Illustrative example of the stochastic wind model.

2.4.3 Affine Model

The linear model presented in the previous section is expressed in deviation variables(also called relative or incremental). From now on and for a matter of comfortingly the system is expressed in affine way. That way all the variables are in absolute values and there is no need to add or subtract the steady states. The procedure how to get the affine model from the deviation one is done in equations 2.50 to 2.55 as shown in (Gosk, 2011).

$$\dot{x} - x^* = A(x - x^*) + B(u - u^*) + E(v - v^*) \tag{2.50}$$

$$y - y^* = C(x - x^*) + D(u - u^*) \tag{2.51}$$

Organizing all the steady values it can be obtained

$$\dot{x} = Ax + Bu + Ev \underbrace{-Ax^* - Bu^* - Ev^* + x^*}_{d_x} \tag{2.52}$$

$$y = Cx + Du \underbrace{-Cx^* - Du^* + y^*}_{d_y} \tag{2.53}$$

then the system can be expressed like

$$\dot{x} = Ax + Bu + Ev + d_x \tag{2.54}$$

$$y = Cx + Du + d_y \tag{2.55}$$

2.5 Model Analysis

In this section the characteristic of the model obtained are studied and the linear model obtained is compared with the non-linear one to verify its behaviour.

2.5.1 Characteristics of the System

2.5.1.1 Stability

The inverted pendulum turbine is inspired in the typical control problem of the inverted pendulum. It is well known that the inverted pendulum is an unstable system and it sounds reasonable that the inverted pendulum turbine may also be unstable.

From (Slotine and Li, 1991) it is known that given a a non-linear system, like the current case, the stability of this system can be discussed from the linearization state space description. This method is known as *Lyapunov's linearization method*. Depending on the eigenvalues of the linearized state space system matrix the stability of the system can be discussed as follows

- If $Re(\lambda_i) < 0 \ \forall i \rightarrow$ The non-linear system is local asymptotic stable.
- If $\exists \ \lambda_i|_{Re(\lambda_i)>0} \rightarrow$ The non-linear system is unstable.
- If $\exists \ \lambda_i|_{Re(\lambda_i)=0} \rightarrow$ Nothing can be said about the stability of the non-linear system.

So with a look at the eigenvalue of the space state description it can easily bear out the instability of the system.

From figure 2.21 it can be seen that one eigenvalue, λ_2, is positive in the whole range of wind speed and the instability is now verified.

Having an unstable system sound reasonable because

- If the angle of inclination is bigger than the steady value then the tower would fall forward since the gravity force is higher than the thrust force.
- If the angle of inclination is lower than the steady value then the tower would fall backwards since the thrust force is higher than the gravity force.

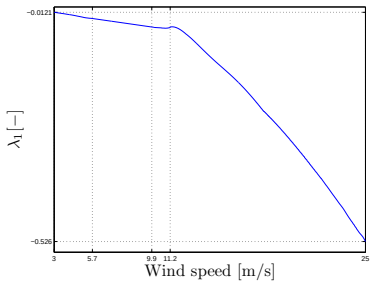

(a) First eigenvalue of the system.

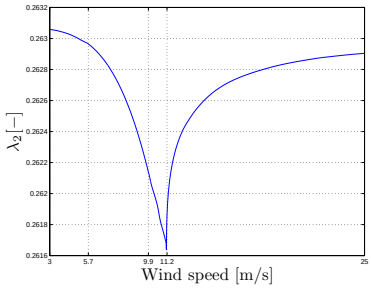

(b) Second eigenvalue of the system.

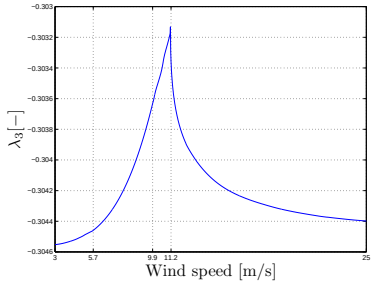

(c) Third eigenvalue of the system.

Figure 2.21: Eigenvalues of the system with respect to the wind.

2.5.1.2 Controllability

From (Skogestad and Postlethwaite, 2005) and (Hendricks et al., 2008) it is known that given a dynamical system

$$\dot{x}(t) = A(t)x(t) + B(t)u(t) \tag{2.56}$$

this system is controllable if for any initial state $x(t_0) = x_0$ there is an input $u(t)$ that brings the system from $x(0) = x_0$ to $x(t_f) = 0$ in a finite time interval. So controllability give an idea how the states are coupled to the inputs. From a more practical point of view the controllability of a system can be verified using the controllability matrix. Given a LTI system

$$\dot{x}(t) = Ax(t) + Bu(t) \tag{2.57}$$

the controllability matrix is defined as follows

$$Mc = \begin{bmatrix} B & AB & A^2B & ... & A^nB \end{bmatrix} \tag{2.58}$$

The system 2.57 is controllable if M_c is full rank. The inverted pendulum turbine has been proved to be controllable since the controllability matrix is full rank for all the wind speed range.

2.5.1.3 Observability

From (Skogestad and Postlethwaite, 2005) and (Hendricks et al., 2008) it is known that given a dynamical system

$$\dot{x}(t) = A(t)x(t) + B(t)u(t) \tag{2.59}$$

$$y(t) = C(t)x(t) + D(t)u(t) \tag{2.60}$$

this system is observable on the finite time interval $[t_0, t_f]$ if any initial state x_0 is uniquely determined by the output $y(t)$ over the same time interval. From a more practical point of view the observability of a system can be verified using the observability matrix. Given a LTI system

$$\dot{x}(t) = Ax(t) + Bu(t) \tag{2.61}$$

$$y(t) = Cx(t) + Du(t) \tag{2.62}$$

the observability matrix is defined as follows

$$Mo = \begin{bmatrix} C \\ CA \\ CA^2 \\ ... \\ CA^{n-1} \end{bmatrix} \tag{2.63}$$

The system 2.61 and 2.62 is observable if M_o is full rank. The observability of the inverted pendulum turbine has been verified since the rank of the M_o is 3 in all the wind interval.

2.5.2 Model Verification

In this section the linear model obtained is compared with the non-linear one in order to verify the reliability of the model. In that purpose the non-linear model and the linear one are compared when into the system step responses in the pitch β, generator's torque T_g and wind speed v are introduced.

Figure 2.22 represents the comparison method. Notice that without an active control on the system the inclination θ and the speed of inclination $\dot{\theta}$ cannot be compared due to the instability of the system. So with the method described above it is just possible to compare the rotational speed ω_r and the electrical power P_e.

In figure 2.23 the different inputs can be seen. Notice that for all the inputs there is a positive step change and a negative one. In the generator torque plot the units are in incremental values referenced into the steady value. The state space description used is for the linearization point of 15 m/s.

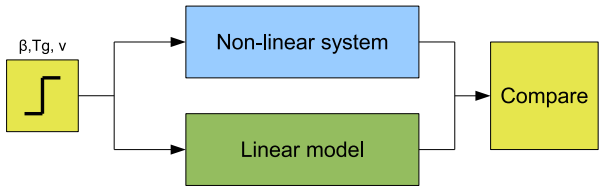

Figure 2.22: Model verification for P_e and ω_r block diagram.

From figure 2.24 it can be seen that the state space description is behaving as it should. The maximum deviation between the linear model and the non-linear for the electrical power is 0.78% of the non-linear value when there is a positive step in the generator torque and for the rotational speed is 0.75% when there is a negative step in the pitch. All this values are small enough to rely on the obtained linear model of the rotor.

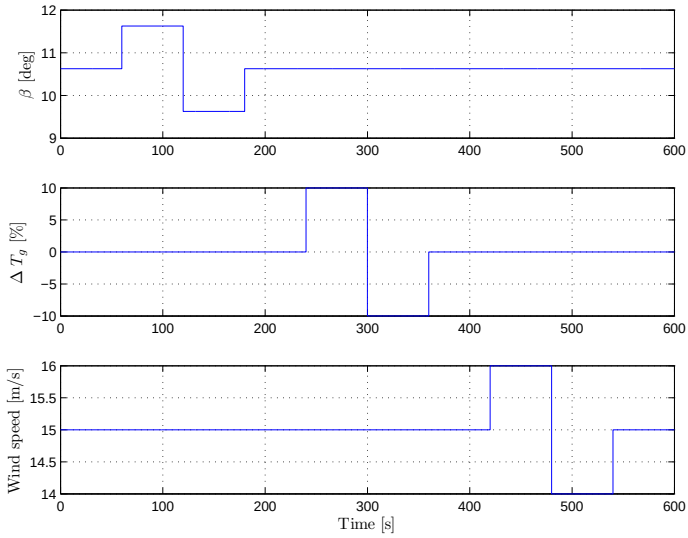

Figure 2.23: Model verification inputs.

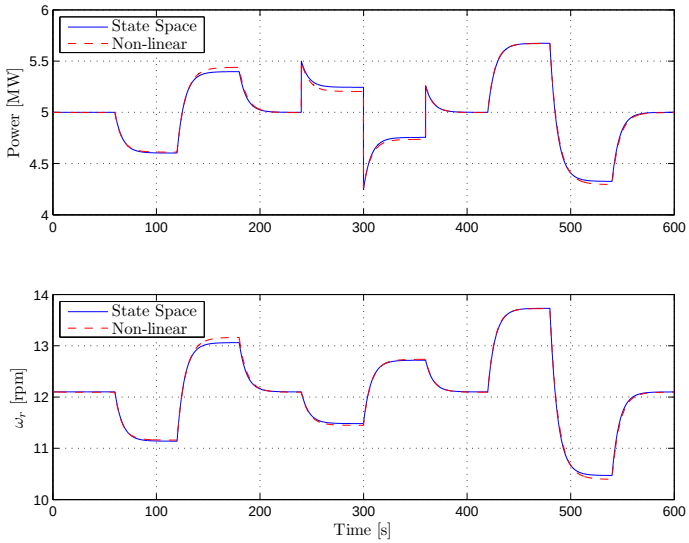

Figure 2.24: Model verification P_e and ω_r.

Now it is time to verify the model of the hinge tower. In order to do that an active control is placed as shown in figure 2.25. In this case just wind steps are introduced to the system.

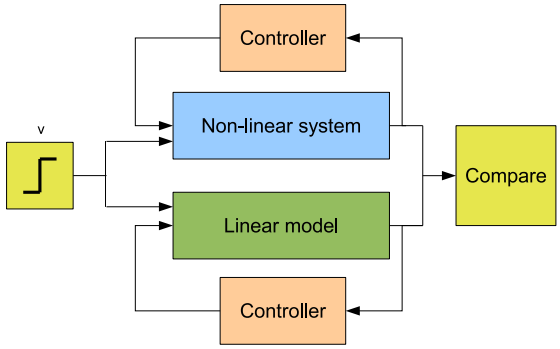

Figure 2.25: Tower model verification block diagram.

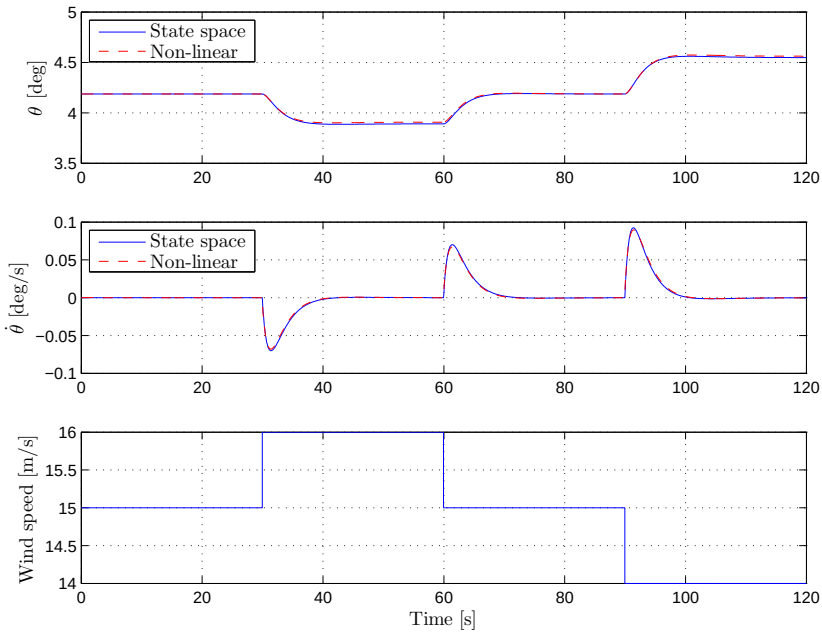

Figure 2.26: Model verification θ and $\dot{\theta}$.

From figure 2.26 it can be seen that the model of the tower is behaving properly. The maximum deviation between the linear model and the non-linear one for θ is 0.4% of the non-linear value when a positive step in the wind is done, while in $\dot{\theta}$ is 3% of the non-linear value when there is a negative step in the wind. In this last case the deviation is a little bit bigger since the values of the speed of inclination are very small. All this values are small enough to rely on the obtained linear model of the hinge tower.

Chapter 3

Control Methods

In this chapter all the control theory used in the realization of this project is explained. The reader should no expect a large and broad discussion of all the concepts introduced.

3.1 Kalman Filter

In this section it is shown the theory behind the estimation of the states, x, by observing the outputs y with an optimal observer: a *Kalman Filter*.

In real applications almost all the measurements done have some errors. This is caused because the states or their measurement may be corrupted by some kind of noise. In that situation it becomes very useful an optimal estimator, like the Kalman filter, that is able to estimate the states with the noisy measurements of them.

The formulation of the optimal observer is done in discrete time but it can also be done in continuous time. This approach is described in detail in (Hendricks et al., 2008).

Before starting the explanation some nomenclature notes should be done:

- The symbol ' ˆ ' means estimated value. So $\hat{x}$ is the estimated value of x and $\hat{y}$ is the estimated value of y.
- y_m is the measured output from the real plant.
- $\hat{x}_{k|k-1}$ is the estimated value of x for the sample k with the data from the sample $k-1$.
- L is the Kalman gain matrix.

Given the LTI system in discrete time

$$x_{k+1} = Ax_k + Bu_k + w_k \tag{3.1}$$

$$y_k = Cx_k + Du_k + v_k \tag{3.2}$$

where w_k is the state noise and v_k is the measurements noise. Both, w_k and v_k are white noise, uncorrelated and normally distributed with zero mean

$$w_k \in N(0, Q_e) \tag{3.3}$$

$$v_k \in N(0, R_e) \tag{3.4}$$

The steady-state Kalman filter is able to estimate the state in two steps the *data update*, equation 3.5, and the *time update*, equation 3.6,

$$\hat{x}_{k|k} = \hat{x}_{k|k-1} + L(y_m - \underbrace{(C\hat{x}_{k|k-1} + Du_k)}_{\hat{y}}) \tag{3.5}$$

$$\hat{x}_{k+1|k} = A\hat{x}_{k|k} + Bu_k \tag{3.6}$$

For a better understanding of how the Kalman filter works in figure 3.1 there is helpful block diagram.

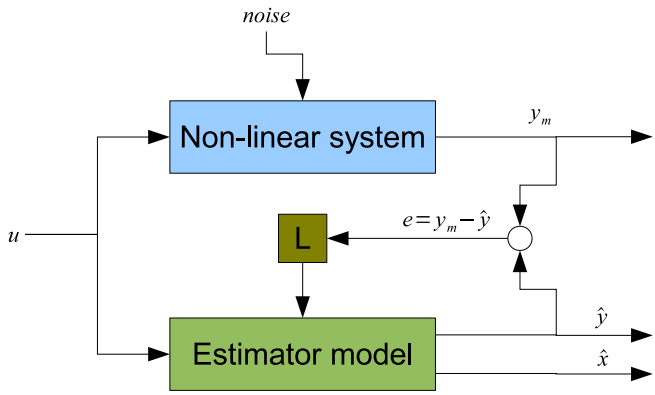

Figure 3.1: Kalman filter block diagram.

In theory the matrices Q_e and R_e are the covariance's matrices of the states and the measurements respectively. If there is information about this covariances matrix then it should be used. In practice since there is no information about this matrices they are used as tuning matrices for the estimator.

3.2 Linear Quadratic Regulator

In this section a solution to the standard regulation problem and the most common version of it, the Linear Quadratic Regulator, are presented. In this formulation the cost function is quadratic in the states and the inputs.

From (Hendricks et al., 2008), given a non-linear n-dimensional system like

$$\dot{x}(t) = f(x(t), u(t), t) \tag{3.7}$$

with the initial condition

$$x(t_0) = x_0 \tag{3.8}$$

The objective is to optimize the control in a finite time interval $[t_0, t_1]$. In order to achieve that goal the *performance index* is presented

$$J(u) = \Phi(x(t_1), t_1) + \int_{t_0}^{t_1} L(x(t), u(t), t)dt \tag{3.9}$$

The performance index is composed by two terms. The first term of equation 3.9 is a function that depends on the final state. The second term of the equation 3.9 is a function that depends on the states and the inputs vectors, also called *cost function*. The performance index give an idea of the quality of the control action defined: a large value of J means a bad control while a small value of J a good control.

The general optimal control problem is try to find a control action u(t) for a interval $[t_0, t_1]$ that minimizes the performance index J.

The linear quadratic regulator is the most common formulation for regulation optimal control problem. The LQR problem is presented in discrete time but it can also be formulated in continuous time. For a more generic formulation the cross terms on the cost function are also considered. In (Poulsen, 2012a) there is a detailed demonstration how to solve the minimization problem but here this is not going to be developed, just the results of it are shown.

Given the LTI system in discrete time

$$x_{k+1} = Ax_k + Bu_k \tag{3.10}$$

with the initial condition

$$x_{|k=0} = x_0 \tag{3.11}$$

the cost function to minimize in a finite horizon N is

$$J = x_N^T P x_N + \sum_{k=0}^{N-1} x_k^T Q x_k + u_k^T R u_k + 2x_k^T N u_k \tag{3.12}$$

While minimizing the cost function a recursive discrete time Ricatti equation needs to be solved

$$S_k = Q + A^T S_{k+1} A - (A^T S_{k+1} B + N)(B^T S_{k+1} B + R)^{-1}(B^T S_{k+1} A + N^T) \tag{3.13}$$

With the solution of equation 3.13 the optimal control law is found

$$u_k = -K_k x_k \tag{3.14}$$

with the gain matrix

$$K_k = (B^T S_{k+1} B + R)^{-1}(B^T S_{k+1} A + N^T) \tag{3.15}$$

The development mentioned above is valid for a finite time horizon. The same results can be extrapolated for a infinite horizon. The Riccati equation to solve is now

$$0 = Q + A^T S A - (A^T S B + N)(B^T S B + R)^{-1}(B^T S A + N^T) - S \tag{3.16}$$

The optimal feedback gain matrix is then

$$K = (B^T S B + R)^{-1}(B^T S A + N^T) \tag{3.17}$$

In the formulation of the cost function 3.12 there are three weight matrices, Q, R and N. Having a high weight in a specific variable put more priority at the minimization of that variable than the others while having a low or zero weight in a variable means that the minimization of the specific variable is not important.

In (Franklin et al., 2002) there is a mention to *Bryson's rule*, which give a first choice for the matrices Q, R and N

$$Q_{ii} = \frac{1}{maximum\ acceptable\ value\ of\ x_i^2} \tag{3.18}$$

$$R_{jj} = \frac{1}{maximum\ acceptable\ value\ of\ u_j^2} \tag{3.19}$$

$$N_{ij} = \frac{1}{maximum\ acceptable\ value\ of\ x_i u_j} \tag{3.20}$$

3.3 Linear Quadratic Gaussian Control

In this section it is presented a control method that uses a *Linear Quadratic Regulator* and a *Kalman filter* all together, this kind of control is known as *Linear Quadratic Gaussian Control*.

The name of *LQG* comes from the use of a *Linear* model, a *Quadratic* cost function and a *Gaussian* white process noise to model disturbances and noise. A broad discussion of *LQG* can be found in (Skogestad and Postlethwaite, 2005). The approach below is done in discrete time but it could be done in continuous time.

Given a LTI system with Gaussian white process noise in the states and measurements

$$x_{k+1} = Ax_k + Bu_k + w_k \tag{3.21}$$

$$y_k = Cx_k + Du_k + v_k \tag{3.22}$$

First of all an optimal controller, a Linear Quadratic Regulator, for the linear system above without the Gaussian noise v_k and e_k needs to be found

$$u(t) = -Kx(t) \tag{3.23}$$

The gain matrix K is found with the techniques mentioned in the previous section 3.2.

Once the optimal controller is designed and optimal estimator is used for estimating the states with the measurements. To achieve that goal a Kalman filter is used. Finally the estimation $\hat{x}$ is substituted in the control action

$$u(t) = -K\hat{x}(t) \tag{3.24}$$

As it can be seen, the *LQG* is a pure application of the *separation theorem* since it is possible to assign the eigenvalues from the state feedback and the eigenvalues from the estimator separately.

In order to make all the explanation more clear in the figure 3.2 there is a block diagram of the LQG problem.

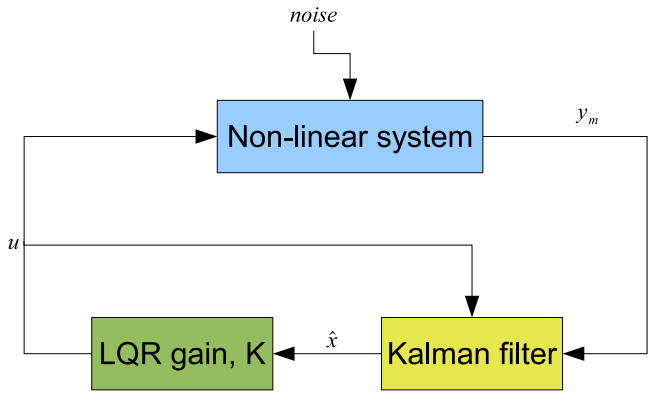

Figure 3.2: LQG problem block diagram.

3.4 Offset-Free Methods

In this section two methods to achieve offset free performance are presented. The first method gets zero offset integrating the difference between the reference value and the real value while the other method introduced disturbances to the model to get offset free performance.

3.4.1 Integral Action

The most easy and old way to get zero offset performance is using an integrator that eliminates the difference between the real and the reference value. When using integrators one have to be aware of their tendency to destabilise a system.

In this project the viability of using an integral action over a LQR problem has been carried out. In (Kedjar and Al-Haddad, 2009) a broad explanation of the linear quadratic regulator with integral action, LQI, can be found.

Given the LTI system in discrete time

$$x_{k+1} = Ax_k + Bu_k \tag{3.25}$$

$$y_k = Cx_k + Du_k \tag{3.26}$$

an integral action to the state x_i is defined

$$e_{k+1} = e_k + (x_{i,k} - x_{i,ref}) \tag{3.27}$$

Then, if the equation 3.27 is added to 3.25 it can be obtained

$$\begin{bmatrix} x_{k+1} \\ e_{k+1} \end{bmatrix} = \begin{bmatrix} A & 0 \\ 0 & I \end{bmatrix} \begin{bmatrix} x_k \\ e_k \end{bmatrix} + \begin{bmatrix} B \\ 0 \end{bmatrix} u_k + \begin{bmatrix} 0 \\ x_{i,k} - x_{i,ref} \end{bmatrix} \tag{3.28}$$

Using also the equation 3.26 the expression above can be reformulated as

$$\begin{bmatrix} x_{k+1} \\ e_{k+1} \end{bmatrix} = \begin{bmatrix} A & 0 \\ C|_{x_i} & I \end{bmatrix} \begin{bmatrix} x_k \\ e_k \end{bmatrix} + \begin{bmatrix} B \\ D|_{x_i} \end{bmatrix} u_k + \begin{bmatrix} 0 \\ -x_{i,ref} \end{bmatrix} \tag{3.29}$$

3.4.2 Disturbance Modelling

Another technique to achieve offset-free performance is to add integrating disturbances to the process model. The aim of adding this disturbances is to eliminate the mismatch between the model and the plant but also the unmeasured disturbances. A broad discussion of the disturbance modelling technique is found in (Pannocchia and Rawlings, 2003) and (Muske and Badgwell, 2002).

The main idea of the disturbance modelling is that the disturbances added to the system absorb any mismatch until zero offset is achieved. The first step to follow when implementing this offset free technique is to add disturbances to the system, afterwards the states and the disturbances are estimated using a Kalman filter designed for the augmented system. When the control loop is closed the disturbances estimations are use to achieve the zero offset performance.

Given the LTI system in discrete time with Gaussian noise

$$x_{k+1} = Ax_k + Bu_k + w_k \tag{3.30}$$

$$y_k = Cx_k + Du_k + v_k \tag{3.31}$$

The disturbances can be placed either in the states, also called inputs disturbances,

$$x_{k+1} = Ax_k + Bu_k + B_d d_k + w_k \tag{3.32}$$

$$d_{k+1} = d_k + w_{k_d} \tag{3.33}$$

either in the measurements, also called outputs disturbances,

$$y_k = Cx_k + Du_k + C_d p_k + v_k \tag{3.34}$$

$$p_{k+1} = p_k + v_{k_p} \tag{3.35}$$

either in both states and measurements

$$\begin{bmatrix} x_{k+1} \\ d_{k+1} \\ p_{k+1} \end{bmatrix} = \begin{bmatrix} A & B_d & 0 \\ 0 & I & 0 \\ 0 & 0 & I \end{bmatrix} \begin{bmatrix} x_k \\ d_k \\ p_k \end{bmatrix} + \begin{bmatrix} B \\ 0 \\ 0 \end{bmatrix} u_k + \begin{bmatrix} w_k \\ w_{k_d} \\ v_{k_p} \end{bmatrix} \tag{3.36}$$

$$y_k = \begin{bmatrix} C & 0 & C_d \end{bmatrix} \begin{bmatrix} x_k \\ d_k \\ p_k \end{bmatrix} + Du_k + v_{k_p} \tag{3.37}$$

where the w_{k_d} and v_{k_p} are the noise of the input and output disturbances respectively.

As mentioned in (Pannocchia and Rawlings, 2003) there are some considerations to take in account to success with the disturbance modelling technique. First of all the augmented system has to be detectable. The detectability of a system is a slightly weaker notion than observability: a system is detectable if and only if all of its unobservable modes are stable. This condition is held if and only if

- The non-augmented system is detectable.
- If the condition below is hold

$$rank \begin{bmatrix} A - I & B_d & 0 \\ C & 0 & C_d \end{bmatrix} = n_x + n_d \tag{3.38}$$

That implies that the maximum number of disturbances that can be added to the system is equal to the number of measurements

$$n_d \leq n_y \tag{3.39}$$

Deciding the structure of the augmented system is not an easy task. There are many things to take in account:

- The number of disturbances.
- Where to place the disturbances in the states and/or in the measurements.
- Chose the appropriate matrices B_d and C_d.
- Check that the conditions mentioned earlier hold.

This is a trial-error method until zero offset performance is achieved. When one accomplish this goal the augmented system is properly designed.

Chapter 4

Implementation and Results

In this chapter the controller implemented and all the results from the simulations are shown. All the control techniques used have been explained in the previous chapter.

First of all the baseline controller implemented by *NREL* in (Jonkman et al., 2009) is explained. Then the control strategy of the implemented controller is exposed and afterwards the results of this control action are shown. Finally the performance of the controller designed over the inverted pendulum turbine is compared with a wind turbine with a stiff tower.

4.1 Baseline Controller

Current wind turbines use quite simple controllers. In this section the baseline controller designed by *NREL* is explained.

The main control objective of the baseline controller is to control the produced electrical power. To achieve that goal two independent controllers are implemented: a generator torque controller and a pitch angle controller.

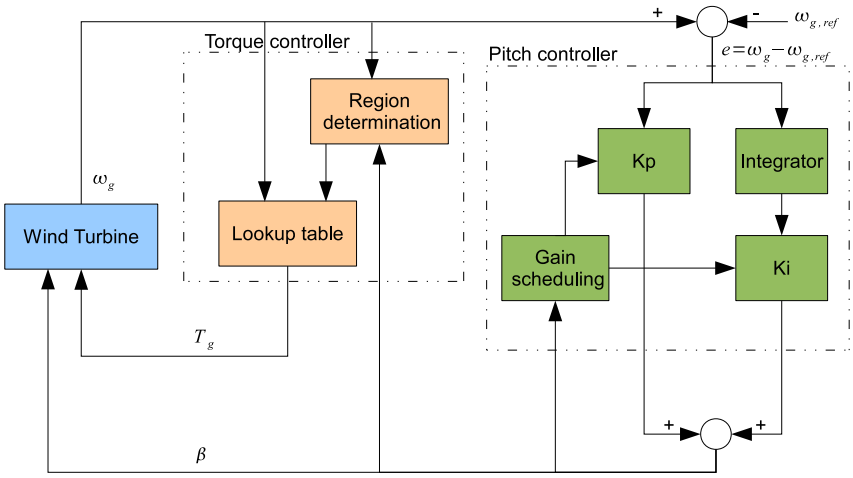

Figure 4.1: Baseline controller flowchart.

The generator torque controller is responsible of controlling the power production below the critical wind speed. The critical wind speed is the one in between the high region (III) and the top region (IV) defined in section 2.3.1 as v_3. The control action of this controller works with a lookup table. Depending on the pitch value and the generator speed the controller identifies the current region and applies the relevant generator torque. Above the critical wind speed the generator torque is kept constant.

The pitch angle controller is responsible of controlling the power produced above the critical wind speed. This is a PI controller with gain scheduling designed on the first order model of the wind turbine. The controller input is the difference between the real generator speed and the rated referenced generator speed. Depending on the pitch angle the gain of the PI controller changes. Below the critical wind speed the pitch angle is kept constant.

In figure 4.1 there is a block diagram of the baseline controller to help to understand how does it work. It is important to notice that this is a basic explanation of the baseline controller and some of the control details have been omitted. In (Jonkman et al., 2009) there is a detailed explanation of a baseline controller for the 5-MW reference wind turbine.

4.2 Control Strategy

The inverted pendulum turbine is an unstable system as demonstrated in section 2.5.1.1. The control objectives of the inverted pendulum turbine are a little bit different from other wind turbines. The main control objective is to keep the tower still, in a suitable inclination. Once the first control objective is accomplished the other goal to achieve is the maximization of the produced electrical power.

In section 2.3 the criteria of how to get the steady state points is explained. The steady states points have been chosen with the aim of maximize the electrical power, like other wind turbines. Once the steady points have been found the inclination of the tower has been chosen accordingly. The criteria followed ensures the maximization of the electrical power.

4.2.1 Control Objectives per Region

Each one of the four regions defined has different control objectives. In this section the control designed for each region is explained.

It is important to notice that in the baseline controller the pitch is kept in a constant value for region I, II and III. This is due to the fact that, between other reasons, the pitch component of the input matrix B is zero since the derivative of the C_p against the pitch angle β is zero.

In the inverted pendulum turbine the pitch component of the input matrix is not zero since the derivative of the C_t curve against the pitch β is not zero. The plots of the derivatives of the C_p and C_t against β and λ are shown in 2.15 and 2.16.

$$B = \begin{bmatrix} \frac{\rho_a \pi R^2 v^3}{2J\omega_r} \frac{\partial C_p(\lambda,\beta)}{\partial \beta} & \frac{-N}{J} \\ 0 & 0 \\ \frac{-\rho_a R^2 \pi v^2}{2M_t^a} \frac{\partial C_t(\lambda,\beta)}{\partial \beta} & 0 \end{bmatrix} \tag{4.1}$$

Low region (I)

In this region the rotation speed is kept in its lowest level while the produced electrical power is maximized. Notice that the criterion followed in the base-

line controller, keeping the pitch angle fixed, cannot be applied in the inverted pendulum turbine. If the pitch is fixed in an certain angle there is no action to keep the tower in an appropriate inclination. So the reference introduced to the system is

$$r = \begin{bmatrix} \omega_r \\ \theta \\ \dot{\theta} \end{bmatrix} = \begin{bmatrix} \omega_{r_{min}} \\ \theta_{ref} \\ 0 \end{bmatrix} \tag{4.2}$$

Mid region (II)

In region II the objective is to maximize the produced electrical power by trying to keep the wind turbine on the top part of the C_p curve. In order to achieve this goal the pitch reference is kept at the optimal point β^* and the ω_r is chosen in a way that the λ is kept at its optimal point λ^*.

$$r = \begin{bmatrix} \omega_r \\ \theta \\ \dot{\theta} \end{bmatrix} = \begin{bmatrix} \frac{\lambda^* v}{R} \\ \theta_{ref} \\ 0 \end{bmatrix} \tag{4.3}$$

High region (III)

In region III the rotational speed reference is kept at its rated value. Since this region is really narrow it has been used for a transition between regions II and IV.

$$r = \begin{bmatrix} \omega_r \\ \theta \\ \dot{\theta} \end{bmatrix} = \begin{bmatrix} \omega_{r_{rated}} \\ \theta_{ref} \\ 0 \end{bmatrix} \tag{4.4}$$

Top region (IV)

In region IV the rotational speed reference is kept at its rated value as the generator torque. Since the objective is to keep the produced electrical power at its rated value the reference pitch angle is increasing, this action is known as *pitching out*.

$$r = \begin{bmatrix} \omega_r \\ \theta \\ \dot{\theta} \end{bmatrix} = \begin{bmatrix} \omega_{r_{rated}} \\ \theta_{ref} \\ 0 \end{bmatrix} \tag{4.5}$$

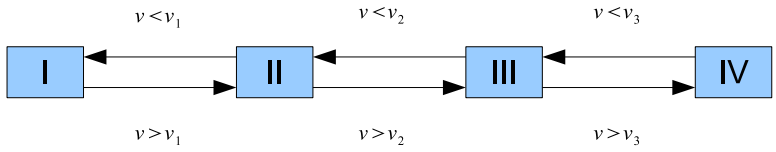

Figure 4.2: Region switching criteria.

4.2.2 Switching Criteria

The criteria chosen for switching between the regions is based on thresholds of the estimated wind. Depending on this estimation the controller knows the current region. Therefore having a good estimation of the wind is crucial. The method followed to get a good wind estimation is explained in 4.3.2.1.

One can be wondering why this criteria is based on the estimated wind and not on the measurement of it. The answer to this question is found in (Xin et al., 1997). The main reason is that it is not possible to measure the effective wind speed which is flowing through the blades due to the stochastic spatial variations in the wind speed on the rotor plane. Using a sensor in that propose does not help either. Wind turbines use anemometers to measure the wind speed. This sensors are placed on top of the nacelle, behind the rotor blades. This position makes that the presence of the turbine itself disturbs the wind measurement. Therefore this sensor should be placed in a separate site where the wind speed measured would be precise enough. Even considering the possibility of the new ubication the rotor plane is huge compared with the wind sensor and any measure obtained with them is not reliable. There are other wind sensors like the ones based on LIDAR technology. This sensors cannot compete, right now, with anemometers since they are expensive and not robust enough. In (Mirzaei et al., 2012a) and (Madsen and Filsø, 2012) there is an interesting use of this technology over a wind turbine. Since one cannot rely on the wind speed sensors the wind experienced by the rotor is estimated using the the wind turbine itself as a wind measuring device.

Besides the switching criterion based on the estimated wind some other considerations should be made. Due to the fact that region III is very narrow and the transition between region III and IV is not easy to handle the region III has been used as a transition between the mid region and the top region. The controller

has been tuned in order to achieve soft transitions between the regions.

4.2.3 Control Strategy Summary

Compared to other control problems the wind turbines dynamics are driven by a disturbance: the wind speed. Beside other variables, the wind speed is one of the main variables to select the operating conditions of wind turbines, like shown in section 2.3.

As it has already been mentioned in the previous section there are four different operation modes of a wind turbine and each of them has different characteristics. A good way of handling this variation in the operating conditions is using a control strategy like the gain scheduling.

In this project to regulate the inverted pendulum turbine, the technique used is based on a gain scheduling LQG controller which is able to compensate the non-linearities inherent in wind turbines.

When using gain scheduling technique some variables are used to decide the current operating point. In the baseline controller explained in section 4.1 the pitch angle and the generator rotational speed are used as scheduling variables. In other studies like (Hammerum, 2006) the gain scheduling variables used are the produced electrical power, the pitch and the generator rotational speed.

In this project the chosen schedule variable is the wind speed which has the advantage that this variable by itself can be used over the entire operating range.

In order to have a good performance of the control action it is necessary to have a precise and reliable value of the effective wind speed. Since there are no accurate measurements of the wind speed available using sensors the wind needs to be estimated. Because of that having a reliable estimation of the wind is very important to have a good performance since the estimated wind speed is used to determine the operating point.

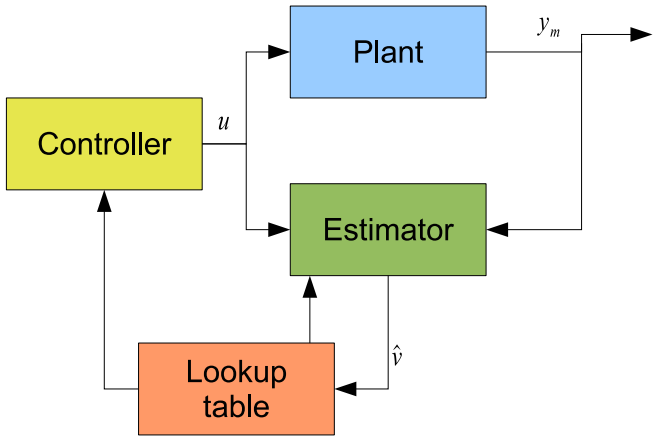

Figure 4.3: Control strategy summary for the inverted pendulum turbine.

From a more practical point of view a lookup table with the linear model, the controller and the observer per each wind speed is defined. So each sample time the estimated wind speed is checked. Then the linear model, the controller and the observer are changed accordingly. In the figure 4.3 a block diagram of the control strategy is shown.

4.3 Control Implementation

4.3.1 Discrete Model

The mathematical model of the inverted pendulum turbine has been presented in continuous time. Since all the simulations are done in discrete time the system needs to be discretized. The chosen sampling time is $T_s = 0.05s$, which give a sampling frequency $f_s = 20Hz$.

When modelling a wind turbine one of the components with faster time constant is the generator torque actuator. From (Henriksen, 2007) the time constant of this actuator is $\tau = 0.1s$. Following the well-known sampling criteria of Nyquist, that can be found in (Proakis and Manolakis, 2007), the sampling time has been chosen to be half of the fastest time constant

$$T_s = \frac{\tau}{2} = 0.05s \tag{4.6}$$

In this thesis the model of the generator torque actuator is not used but thinking on possible future changes it has been decided the sampling time of 0.05s.

The method used to discretise the system is the well-known *zero order holding*. This method has the peculiarity that in the sample points the discrete value and the continuous one are equal, then the discrete value is kept constant until the next sample point where both signals, the continuous and the discrete, are equal again. This method has been used since is a proven method that on systems with time constants larger than two times the sampling time, like the current one, give good results.

4.3.2 Wind and States Estimation

4.3.2.1 Wind Estimation

In this project having a good estimation of the wind is really important since depending on that the control action applied to the system is different. In (Østergaard et al., 2007) there is an interesting approach of how to estimate the wind speed but the technique used in this project is extracted from (Xin et al., 1997) where a broad explanation can be found.

To get a good estimation of the wind the model of the inverted pendulum turbine has been extended with two new states: the wind speed v and the wind acceleration $\dot{v}$.

Having the state space description of the inverted pendulum turbine

$$\dot{x} = Ax + Bu + Ev + d_x \tag{4.7}$$

$$y = Cx + Du + d_y \tag{4.8}$$

and the state space description of the stochastic wind

$$\begin{bmatrix} \dot{v}_t \\ \ddot{v}_t \end{bmatrix} = \underbrace{\begin{bmatrix} 0 & 1 \\ \frac{-1}{p_1 p_2} & \frac{-p_1-p_2}{p_1 p_2} \end{bmatrix}}_{A_w} \begin{bmatrix} v_t \\ \dot{v}_t \end{bmatrix} + \begin{bmatrix} 0 \\ \frac{k}{p_1 p_2} \end{bmatrix} e \tag{4.9}$$

$$e \in N(0,1) \tag{4.10}$$

then the extended model is

$$\begin{aligned} \dot{x}_e &= A_e x_e + B_e u_e + d_{xe} && (4.11) \\ y_e &= C_e x_e + D_e u_e + d_{ye} && (4.12) \end{aligned}$$

where

$$A_e = \begin{bmatrix} A_{[3x3]} & E_{[3x1]}\ 0_{[3x1]} \\ 0_{[2x3]} & A_{w_{[2x2]}} \end{bmatrix} \qquad B_e = \begin{bmatrix} B_{[3x2]} \\ 0_{[2x2]} \end{bmatrix} \qquad d_{xe} = \begin{bmatrix} d_{x[3x1]} \\ 0_{[2x1]} \end{bmatrix} \tag{4.13}$$

$$C_e = \begin{bmatrix} C_{[3x3]} & 0_{[3x2]} \end{bmatrix} \qquad D_e = \begin{bmatrix} D_{[3x2]} \end{bmatrix} \qquad d_{ye} = \begin{bmatrix} d_{y[3x1]} \end{bmatrix} \tag{4.14}$$

$$x_e = \begin{bmatrix} x_{[3x1]} \\ v_{[1x1]} \\ \dot{v}_{[1x1]} \end{bmatrix} \qquad y_e = y \qquad u_e = u \tag{4.15}$$

Notice that since it is not possible to control the wind the input matrix has been extended with zeros.

The observability of the extended system have been check with the observability matrix M_o defined in section 2.5.1.3. The rank of M_o is five for the whole wind speed range. That means that all the states of the extended model, including v and $\dot{v}$, can be estimated observing the measurements.

In figures 4.4 to 4.6 the results of using this estimation technique can be seen. In figure 4.4 the estimation of the wind is shown when into the system deterministic steps on the wind are introduced and in figure 4.5 when the stochastic wind is introduced. In figure 4.6 the error of estimation in the stochastic case is shown.

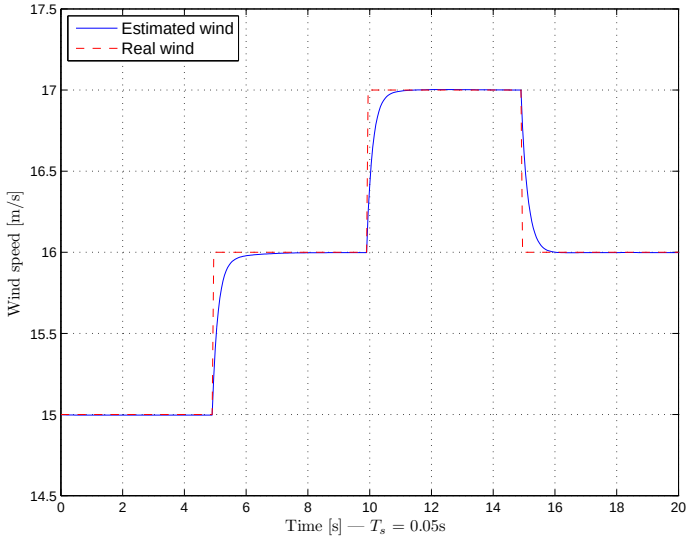

Figure 4.4: Example of wind speed estimation: deterministic steps.

From the deterministic simulation it can be seen that the wind speed estimation is fast, it has a time constant of $\tau = 0.2s$, and precise, the order of magnitude of steady error of estimation is 0.001 m/s.

From the stochastic simulation it can be seen that the wind can be estimated with a good accuracy when having the stochastic wind. The mean value of the error of estimation is 0.0042 m/s and the standard deviation is 0.0485 m/s. The dynamics of the wind turbine change according to the wind. Having an estimation accuracy around 0.1 m/s can reflect all the dynamical changes of the wind turbine with precision. The results shown that the estimation of the wind is not going to be a problem while controlling the system.

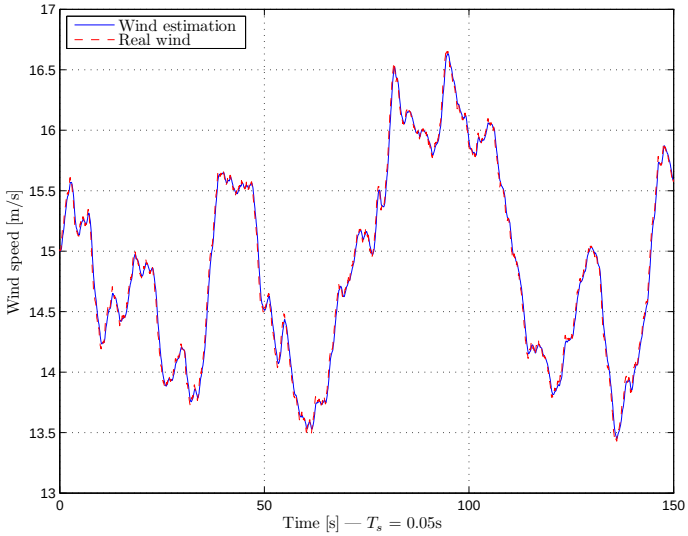

Figure 4.5: Example of wind speed estimation: stochastic wind.

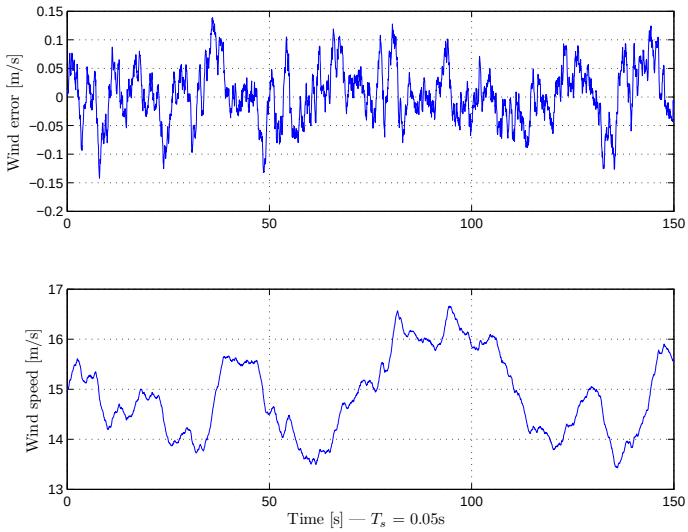

Figure 4.6: Error of wind speed estimation: stochastic wind.

4.3.2.2 States Estimation

Besides having a good estimation of the wind it is also necessary to have a good estimation of the states since depending on this estimation the control inputs are defined.

In figures 4.7 to 4.9 the estimation of the states can be seen. In figure 4.7 the estimation of the states is shown when into the system deterministic steps in the wind are introduced. Notice that the wind introduced into the system is the same as shown in figure 4.4. In figure 4.8 the estimation of the states is shown when into the system the stochastic wind is introduced. In figure 4.9 the error of estimation in the stochastic case is shown. The stochastic wind introduced into the system is the same as shown in the wind estimation case in figure 4.5.

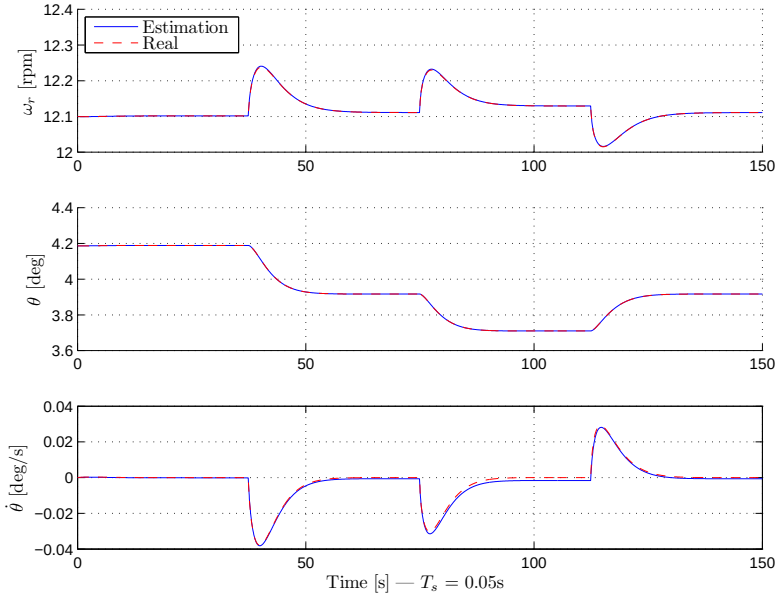

Figure 4.7: Example of states estimation: deterministic wind steps.

As it can be seen from the plots shown the estimation of the states is accurate. The order of magnitude of the error of estimation of ω_r is 0.0001 rpm, of θ is 0.0001 deg and of $\dot{\theta}$ is 0.001 deg/s. The reason of this accuracy is due to the fact that two of the states are also measurements so there is direct feedback from the plant.

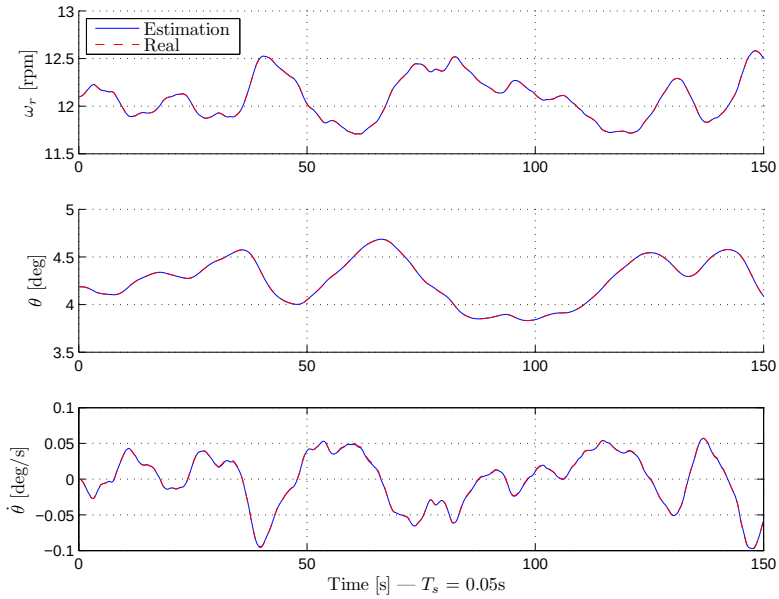

Figure 4.8: Example of states estimation: stochastic wind.

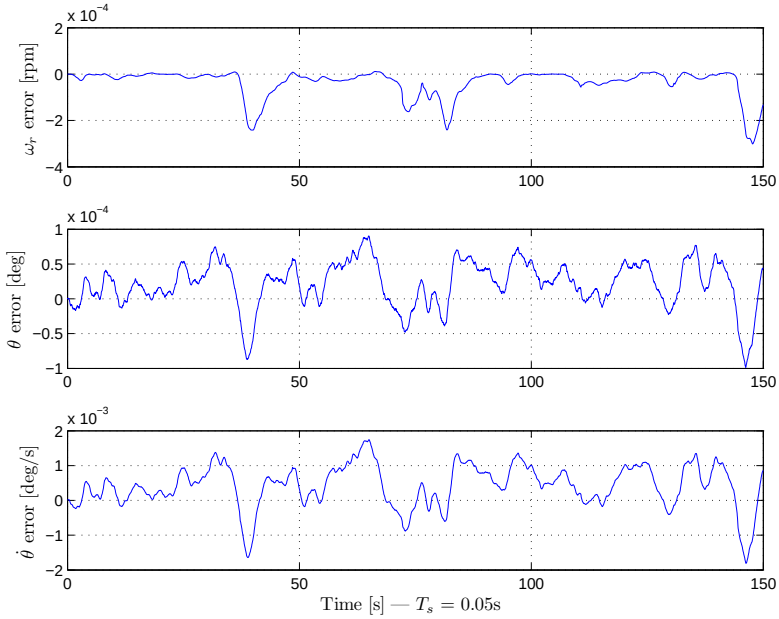

Figure 4.9: Error of states estimation: stochastic wind.

4.3.2.3 Kalman Tuning

As mentioned in chapter 3.1 when designing a Kalman filter the covariance matrix of the states Q_e and the covariance matrix of the measurements R_e is required. The model implemented have two kinds of noise, the noise introduced by the wind model and the noise that appears from comparing a linear model with a non-linear one. When estimating the covariance matrices Q_e and R_e a likelihood function can be used. In this thesis this technique is not used and the covariance matrices have been estimated by hand.

The only data available in this project is the covariance of the wind speed model. This matrix can be obtained with the state space description of the stochastic wind model and by solving a Lyapunov equation. The procedure of how to obtain this matrix, in this report notated as R_w, can be found in (Poulsen, 2012b) but in this report it is not going to be explained.

In this project the covariance matrix of the wind speed model is used as a first guess as follows

$$Q_e = \begin{bmatrix} 0_{[3x3]} & 0_{[3x2]} \\ 0_{[2x3]} & Rw_{[2x2]} \end{bmatrix} + Q_{e,aux} \tag{4.16}$$

where Rw is the covariance matrix of the stochastic wind model.

In equations 4.17 and 4.18 the tuning matrices can be seen while the weight values for each wind speed are shown in the table 4.1. It is important to know that if a value in the table change from one wind speed to another there is a linear interpolation between them.

$$Q_e = \begin{bmatrix} \sigma(\omega_r) & 0 & 0 & 0 & 0 \\ 0 & \sigma(\theta) & 0 & 0 & 0 \\ 0 & 0 & \sigma(\dot{\theta}) & 0 & 0 \\ 0 & 0 & 0 & \sigma(v) & 0 \\ 0 & 0 & 0 & 0 & \sigma(\dot{v}) \end{bmatrix} \tag{4.17}$$

$$R_e = \begin{bmatrix} \sigma(P_e) & 0 & 0 \\ 0 & \sigma(\omega_r) & 0 \\ 0 & 0 & \sigma(\theta) \end{bmatrix} \tag{4.18}$$

Table 4.1: Kalman Filter Weight Values.

v [m/s]	$\sigma(\omega_r)$	$\sigma(\theta)$	$\sigma(\dot{\theta})$	$\sigma(v)$	$\sigma(\dot{v})$	$\sigma(P_e)$	$\sigma(\omega_r)$	$\sigma(\theta)$
3	1e0	1e0	1e0	1e3	1e2	1e-4	1e-4	1e-3
10.5	1e0	1e0	1e0	1e3	1e2	1e-4	1e-4	1e-3
12	1e0	1e0	1e0	5e2	1e1	1e-4	1e-4	1e-3
15	5e1	1e0	1e0	5e4	1e3	1e-4	1e-4	1e-3
25	5e1	1e0	1e0	5e4	1e3	1e-4	1e-4	1e-3

Since the noise introduced by the difference between the linear model and the non-linear one is higher than the noise introduced by the wind the v and $\dot{v}$ component in Q_e is higher than the components from R_w. As an example of how the weights have been obtained the way to get the weight θ in R_e is explained. Knowing that the maximum value of θ is 8.71 degrees and supposing that the sensor used to measure this inclination can make errors around 5% the maximum error of measurement is the 5% of the 8.71 deg, then the covariance value of θ in R_e could be estimated as

$$\sigma(\theta) = 8.71\ deg\ \frac{\pi\ rad}{180\ deg}\ 5\% = 7.6e-3\ rad \approx 1e-3\ rad \tag{4.19}$$

The other components have been tuned by hand in a similar way.

From a practical point of view a high weight on a component in the covariance matrix results as a high priority of having good estimation on that component.

4.3.3 Offset-Free Performance

Without implementing any offset-free method it is expected to have offset performance. In figure 4.10 there is the response when into the system, controlled by a LQG regulator, an step on the wind is introduced.

It can be seen that the control implemented have a small offset. In the electrical power the offset is 0.2 % of the reference value and in the rotational speed is 0.18 % of the reference value.

The two offset-free methods introduced in section 3.4 have been implemented. In the integral action case the integrator is placed in the rotational speed ω_r. It has been proved that just with one integrator the zero offset performance can be achieved for all the regions.

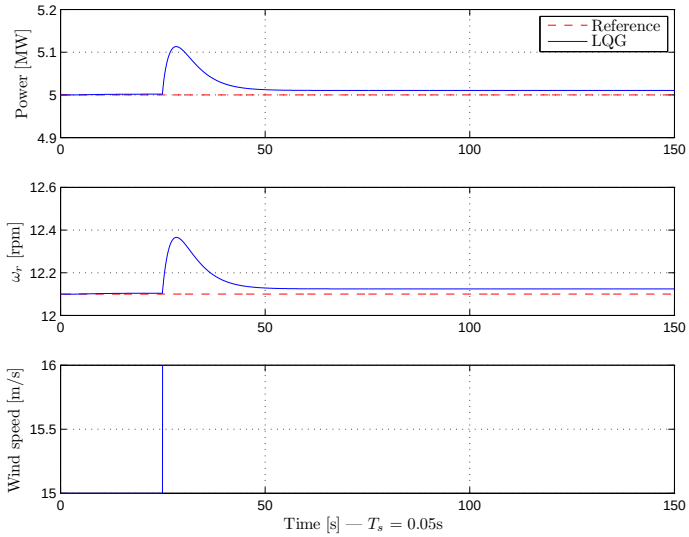

Figure 4.10: Step response on the LQG system.

The disturbance modelling has been implemented over the extended model. It has been proved that just with one input disturbance in the angle of inclination θ the offset free performance is ensured.

In figure 4.11 a comparison between this two offset methods is shown.

From the step response in figure 4.11 it can be seen that both methods ensure offset free performance. It also can be seen that the integral action achieves zero offset before than the disturbance modelling. The undershoot that can be appreciated in the electrical power can be explained as follows: the integrator is placed in the ω_r, when the wind changes the reference of the ω_r increases, this causes a drop in the generator torque which causes the drop in the electrical power.

In the real world the wind is not deterministic. The stochastic wind speed is a more realistic model and before making any decision some stochastic simulations should be done. In order to make it easy to compare all the simulations will be done in region IV. In figure 4.12 the stochastic wind speed introduced to the system to compare both methods is shown. In figure 4.13 the results of the comparison are shown.

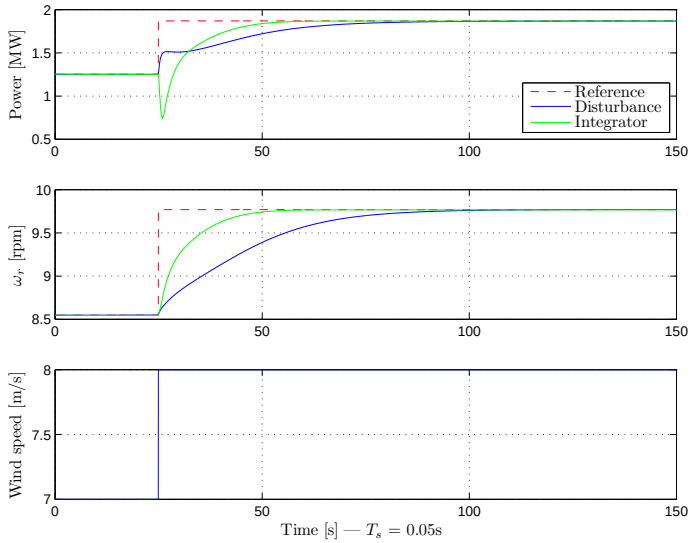

Figure 4.11: Offset-free methods comparison: deterministic wind steps.

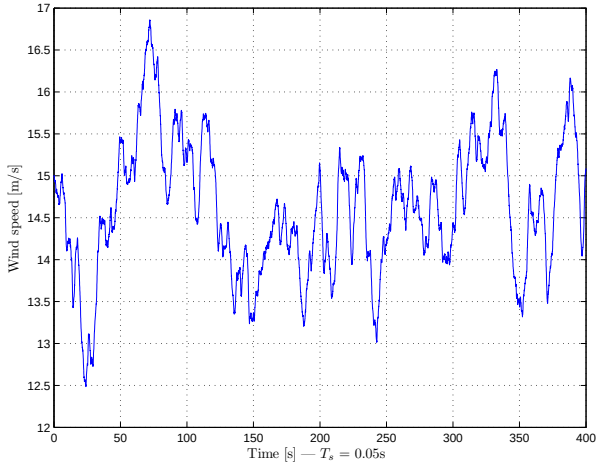

Figure 4.12: Stochastic wind speed introduced for comparison.

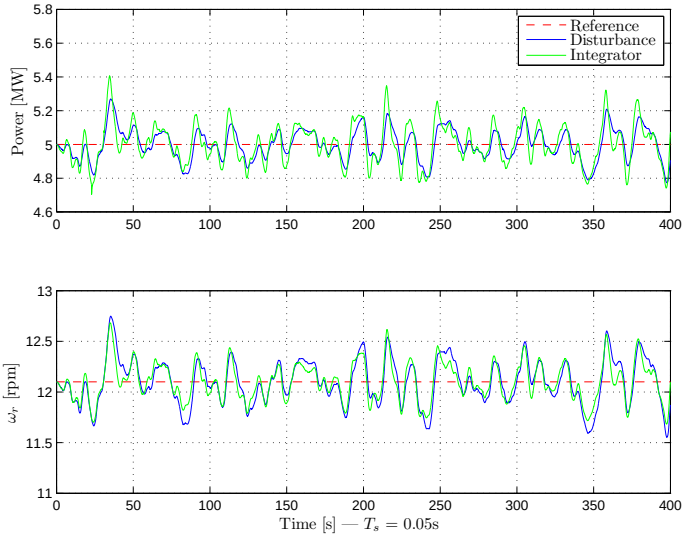

Figure 4.13: Offset-free methods comparison: stochastic wind.

From the figure 4.13 it can be seen that the variation on the electrical power is bigger with integral action than with the disturbance modelling. This result was expected since when introducing a integrator to the system it always tend to make the system unstable. This is inherent to integrators, they are able to eliminated the steady error but they add -90 deg in the phase margin reducing that way the stability of the system. Just with the plots one cannot say which method is better. Ten simulations have been done and some statistical data has been extracted for the two cases. In table 4.2 this statistical data can be found. Notice that there is a comparison of the error of P_e, the error of ω_r and the error of estimation of the wind. The wind estimation has been included on the table because having a good wind estimation is very important in the controller designed.

Table 4.2: Statistical Data for Comparison: Disturbance Vs. Integrator.

Case	mean(P_e)	σ (P_e)	mean(ω_r)	σ (ω_r)	mean($\hat{v}$)	σ ($\hat{v}$)
Integrator	0.0061	0.1124	0.0083	0.1871	0.0049	0.2285
Disturbance	0.0024	0.0948	0.0059	0.2280	0.0178	0.0758

From the statistical data of the table 4.2 one can see that the disturbance modelling has better offset free performance than the integral action since the mean value of the error in the electrical power and in the rotational speed is smaller. When comparing the quality of the estimated wind one is looking

Table 4.3: Statistical Data for Comparison: Disturbance Vs. LQG.

Case	mean(P_e)	σ (P_e)	mean(ω_r)	σ (ω_r)	mean($\hat{v}$)	σ ($\hat{v}$)
LQG	0.0064	0.0943	0.0137	0.2237	0.0027	0.0505
Disturbance	0.0024	0.0948	0.0059	0.2280	0.0178	0.0758

for zero mean and small variation in the error of estimation. The disturbance modelling has a worse mean value but the variation for the integrator is almost 3 times the variation of the disturbance modelling. Having an offset of almost 0.02 m/s in the estimated wind is better than having a standard deviation of 0.23 m/s. Because all this reasons the integral action has been discarded.

Once the integral action has been discarded a comparison between the LQG and the LQG with disturbance modelling is done because sometimes the improvement that an offset free methods achieve does not worth the use of it. The stochastic wind defined in figure 4.12 is use in this comparison. In figure 4.14 the results of the comparison can be seen.

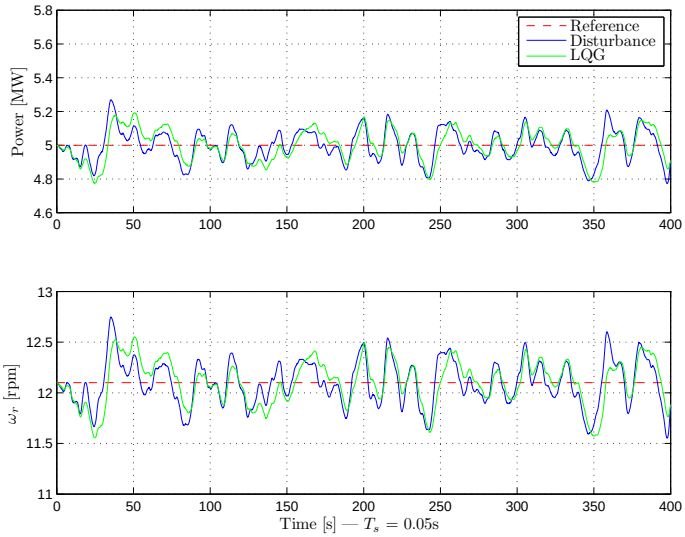

Figure 4.14: Disturbance modelling and LQG comparison: stochastic wind.

From figure 4.14 one cannot decide which method is better since both performances are quite similar. Ten simulations have been done and some statistical data has been extracted in order to compare both methods. All the data can be seen in table 4.3.

From table 4.3 it can be seen that the disturbance modelling has better offset free performance, as expected, but the wind estimation is better in the LQG. This worse estimation is due to the fact that an extra disturbance has been added to the system. Adding a disturbance into the system give more estimation work to the Kalman filter and since the wind is a disturbance into the wind turbine system the estimation of the wind and the estimation of the disturbance fight each other. It is possible to reach zero offset but as a drawback the estimation of the wind is worse. Since having a good estimation of the wind speed is very important and the offset free performance than the disturbance modelling achieves is not much better than the one achieved by the LQG the LQG with disturbance modelling has been discarded and the controller that is going to be used is the LQG without any offset method.

4.3.4 LQG

In this section the LQG control implemented and the results obtained are shown. All the details referring the states and wind estimation have been already shown before so they are omitted in this section. This chapter is focused on the control part of the LQG. In figure 4.15 there is a block diagram of the Linear Quadratic Gaussian Control implemented in the realization of this project with the wind model. In order to show the results of the controller designed two different kinds of simulations are shown: deterministic wind and stochastic wind simulations.

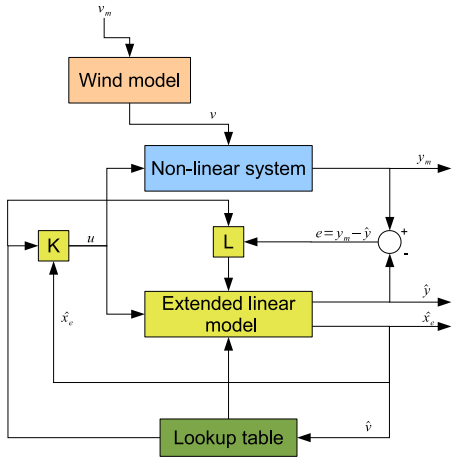

Figure 4.15: LQG complete block diagram.

4.3.4.1 Simulations

In figures 4.16 to 4.19 a simulation with a deterministic step change in the wind is shown.

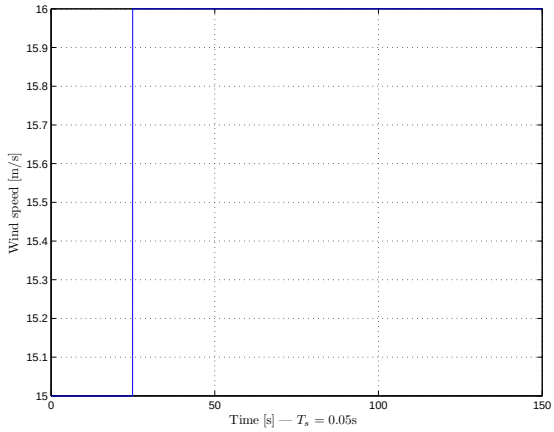

Figure 4.16: Deterministic wind introduced into the system.

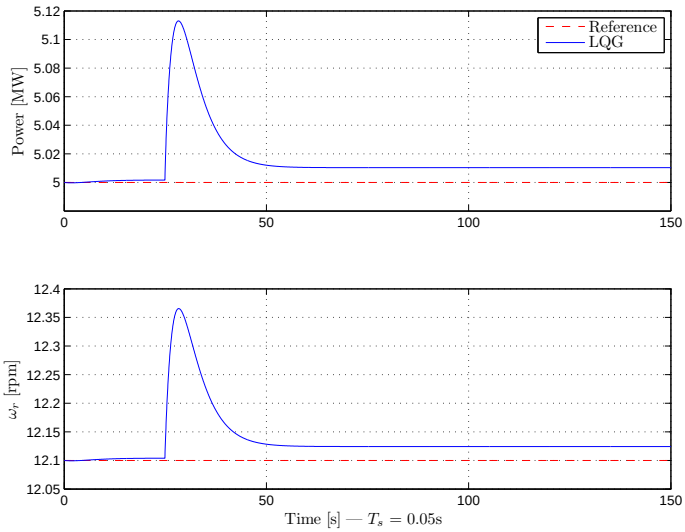

Figure 4.17: Electrical power and rotational speed for deterministic wind.

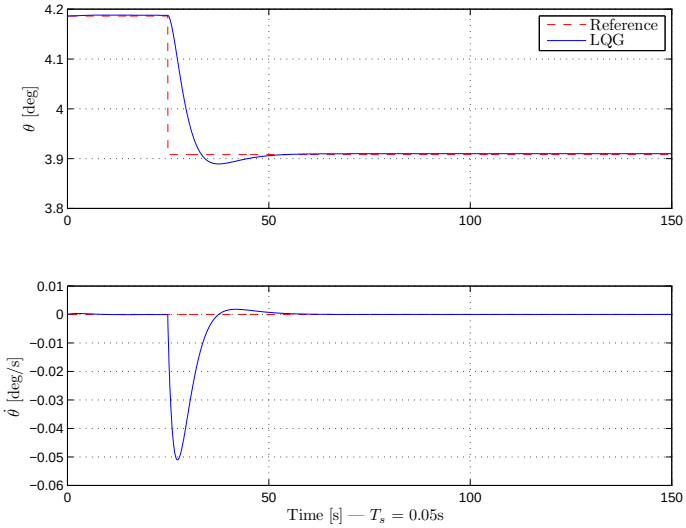

Figure 4.18: Inclination and speed of inclination for deterministic wind.

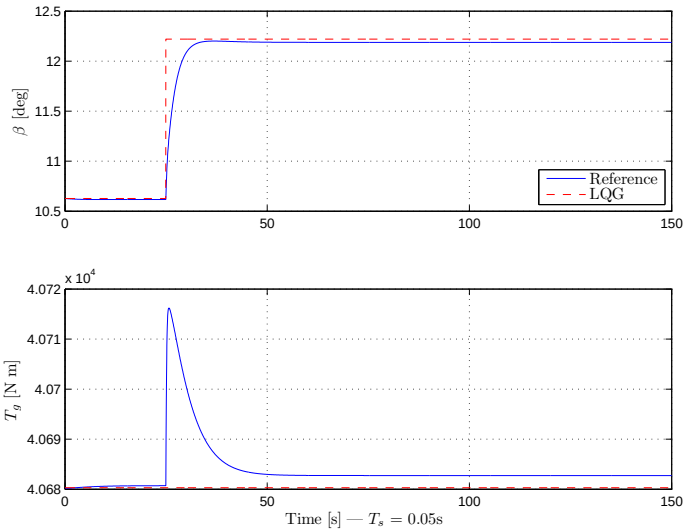

Figure 4.19: Pitch angle and generator torque for deterministic wind.

The deterministic simulations show that there is offset in the controller implemented. This is just reasonable since no offset free control has been introduced. The justification to this fact has already been mentioned in the previous section.

In figures 4.20 to 4.24 a simulation with the stochastic wind is shown. Notice that a whole swept up and down in all the regions has been done.

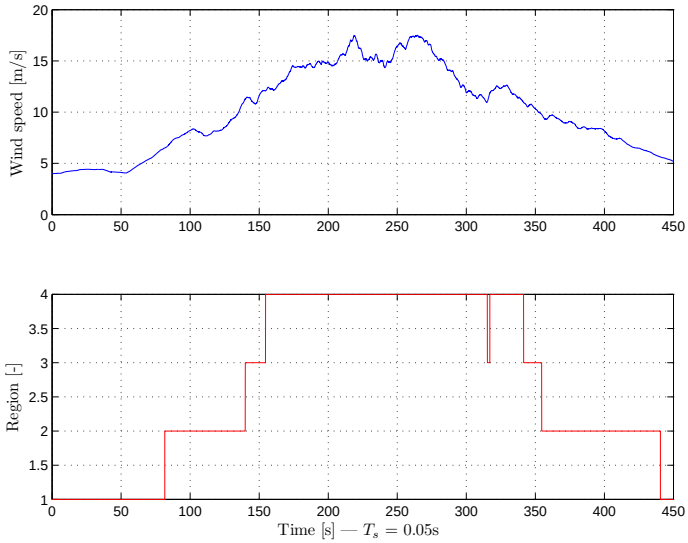

Figure 4.20: Stochastic wind introduced to the system and region definition.

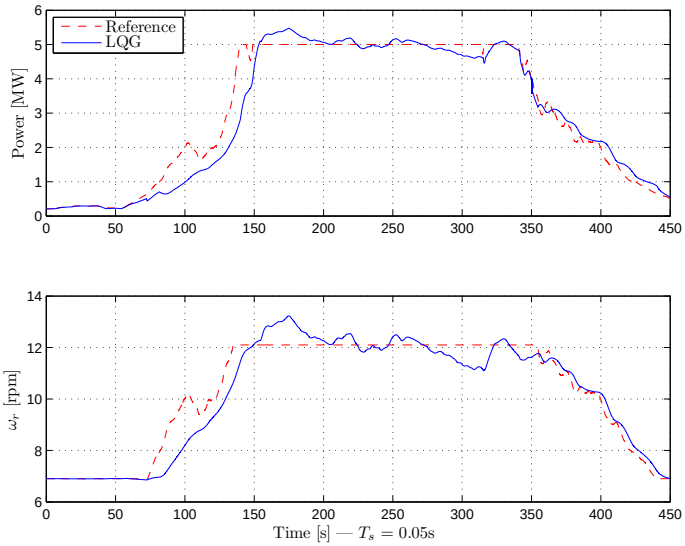

Figure 4.21: Electrical power and rotational speed for stochastic wind.

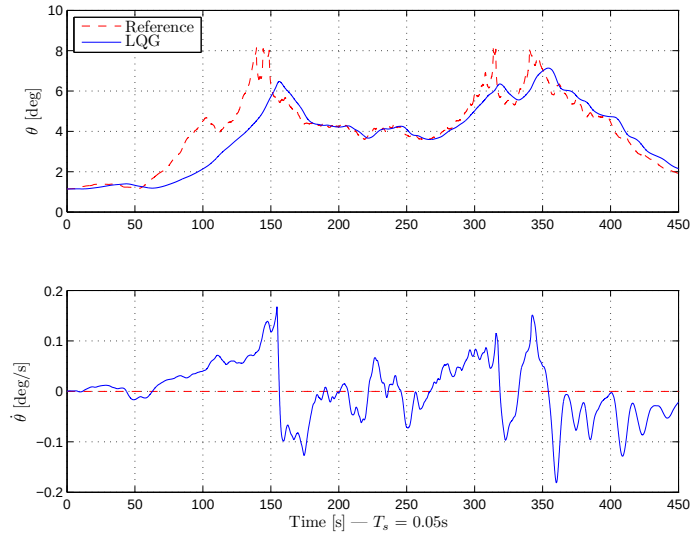

Figure 4.22: Inclination and speed of inclination for stochastic wind.

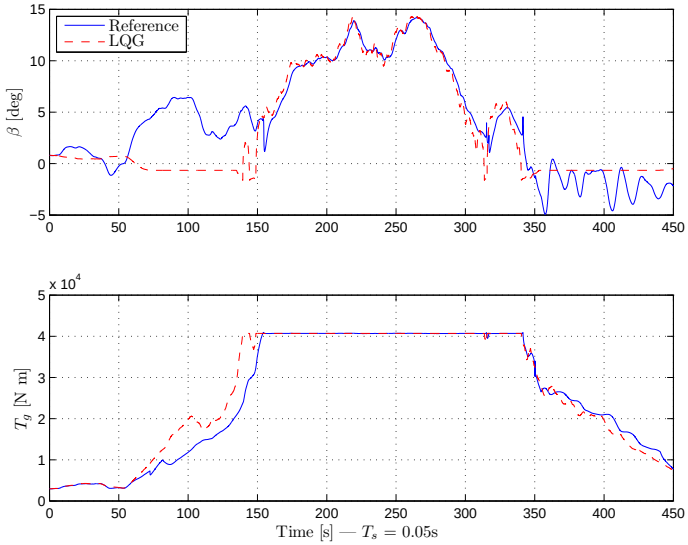

Figure 4.23: Pitch angle and generator torque for stochastic wind.

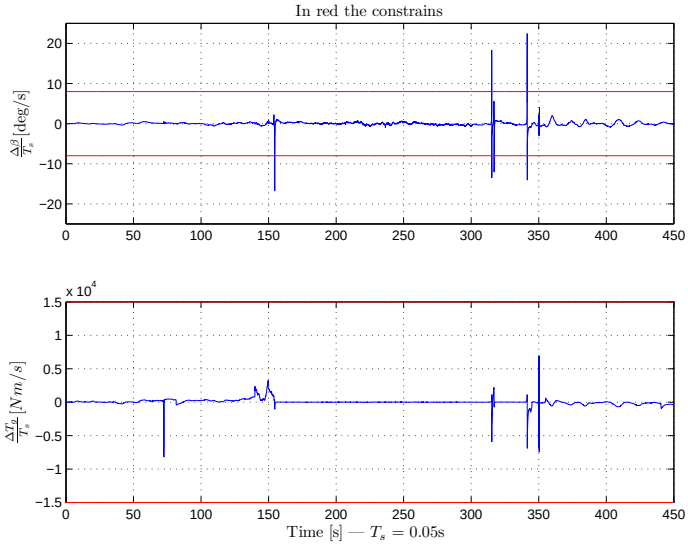

Figure 4.24: Pitch and generator torque derivatives for stochastic wind.

The stochastic simulations show that the there are some problems when switching between regions III and IV. If one looks the derivative of the pitch, in figure 4.24, one can easily see picks when switching form region III to IV and vice versa. One may think that this picks are due to the switching criteria but that is not the reason. When the wind is closer to the critical point (defined in this thesis as v_3) the reference angle of inclination reaches its maximum. So when crossing v_3 there is a drastic change in the speed of inclination, as it can be seen in 4.22, if it was growing then it began to decrease and the other way around. Looking at the inclination angle in figure 4.22 one can see that closer to the critical point the inclination angle is bigger than the reference one, so the tower is about to collapse since the thrust force is not big enough to compensate the gravitational force of the tower. In front of that situation the controller decided to decrease really fast the pitch angle, see in figure 4.23, offering more resistance to the wind and then increasing the thrust force. That way the angle of inclination is reduced until it gets close to the reference value. The same reasoning made before can be done when switching from region IV to III. So the picks in the pitch are cause for the controller to avoid the collapse of the inverted pendulum turbine. The conclusion that one can reach is that with the control implemented in the inverted pendulum turbine the inclination of the tower cannot be kept in the reference value without hitting the constrains on the pitching speed.

The controller can keep good track of the reference in all the regions except the second one. In region II the pitch reference value is constant, but the pitch cannot be fixed otherwise the tower would collapse. This makes it difficult to follow the reference properly. Besides the problem in the critical point the controller is working properly.

4.3.4.2 Controller Tuning

When designing the controller for the LQG problem the three weigh matrices mentioned in section 3.2 need to be defined. The weight matrices used in the design of the controller can be seen in equations 4.20 to 4.22 while the weight value are shown in table 4.4. It is important to know that, like in the Kalman filter tuning, if a value change from one wind speed to another there is a linear interpolation between them.

$$Q = \begin{bmatrix} \omega_r & 0 & 0 & 0 & 0 \\ 0 & \theta & 0 & 0 & 0 \\ 0 & 0 & \dot{\theta} & 0 & 0 \\ 0 & 0 & 0 & v & 0 \\ 0 & 0 & 0 & 0 & \dot{v} \end{bmatrix} \tag{4.20}$$

Table 4.4: Controller Weight Values.

Wind speed [m/s]	ω_r	θ	$\dot{\theta}$	v	$\dot{v}$	β	T_g	$\omega_r T_g$
3	1e1	1e0	1e0	0	0	1e0	1e-1	0
5	1e1	1e0	1e0	0	0	1e0	1e-1	0
6	5e2	1e0	1e0	0	0	1e0	1e2	0
9.9	5e2	1e0	1e0	0	0	1e0	1e2	0
10.5	5e2	1e0	1e0	0	0	1e0	1e2	0
12	5e1	1e0	1e0	0	0	1e4	5e4	2e2
15	5e1	1e0	1e0	0	0	1e2	1e3	7e1
25	5e1	1e0	1e0	0	0	1e2	1e3	7e1

$$R = \begin{bmatrix} \beta & 0 \\ 0 & T_g \end{bmatrix} \tag{4.21}$$

$$N = \begin{bmatrix} 0 & \omega_r T_g \\ 0 & 0 \\ 0 & 0 \\ 0 & 0 \\ 0 & 0 \end{bmatrix} \tag{4.22}$$

Zero weight has been placed in the wind speed and wind acceleration since these two states are uncontrollable. A high weigh has been placed in the rotational speed because keeping a good track of it is crucial for the whole control of the wind turbine. Notice that in region two a higher value has been placed in the rotational speed since in that region is more difficult to follow the reference since the derivative of the C_p against β is zero, like in regions I and III, but the reference value is not constant. To manage the difficult transition between regions III and IV a high value has been placed on the input variables close to the critical point. It is important to know that the only cross term used is the $\omega_r T_g$ which is the electrical power. In order to get a gain matrix K the value of the P_e has to be smaller than a specific value to ensure the existence of a solution. The value chosen for the P_e is the maximum that ensure existence of solution of the LQR problem.

4.4 Comparison

In this section two comparisons are done. The first one compares a wind turbine with a stiff tower controlled by the baseline controller designed by *NREL* and controlled with the LQG designed in this project. The second one compares a wind turbine with a stiff tower and the inverted pendulum turbine both controlled with the same regulator, the LQG designed in this thesis.

The wind turbine with a stiff tower is modelled as a first order system, also known as *WT0*. The differential equation that models the dynamics of this system is

$$J\dot{\omega}_r = \frac{P_r}{\omega_r} - NTg \tag{4.23}$$

which has already been introduced when modelling the rotor of the inverted pendulum turbine.

4.4.1 Baseline Vs. LQG Controller

In this first comparison the model used is the same, the WT0 with stiff tower, while the control action is different. In one case the baseline controller is used and in the other case the designed LQG is used.

In figure 4.25 the stochastic wind introduced to make the comparison in region IV is shown. In figures 4.26 to 4.28 the results are shown.

From figure 4.26 it can be seen that the controller designed is able to keep the electrical power much closer to the reference. The variation on the electrical power and on the rotational speed is much higher for the baseline controller than for the LQG. From figures 4.27 and 4.28 on can see that for the LQG the pitch activity is higher than for the baseline controller. This higher activity explains the ability of the designed controller to keep better track on the electrical power.

To make a comparison in the whole wind range the stochastic wind defined in figure 4.20 is used. The results of this simulation are shown in 4.29. With the data from 4.29 the electricity produced in 450 seconds for the baseline controller is 382 kWh while with the LQG is 384 kWh.

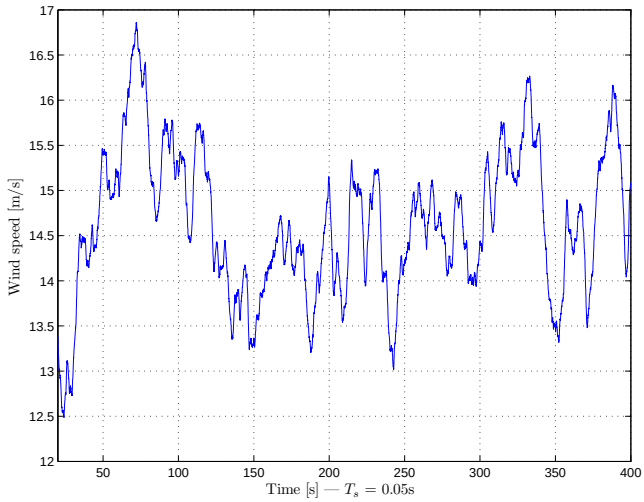

Figure 4.25: Stochastic wind speed for comparison in region IV.

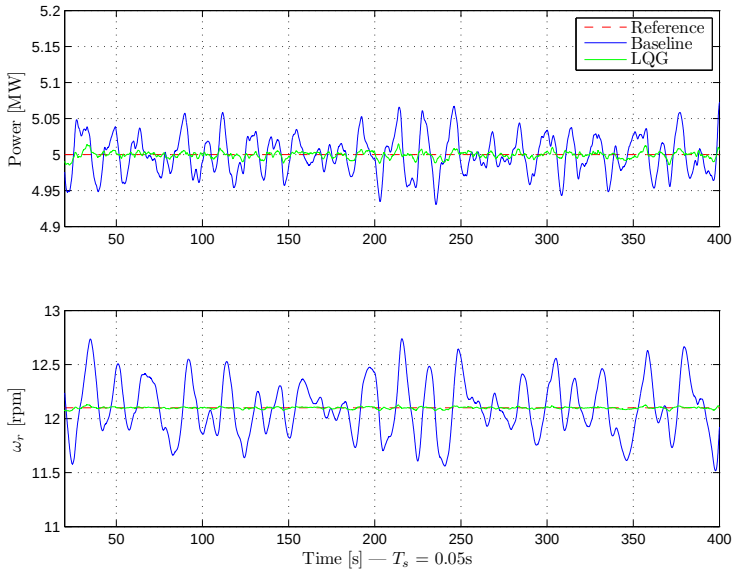

Figure 4.26: Electrical power and rotational speed comparison between baseline and LQG controller in region IV.

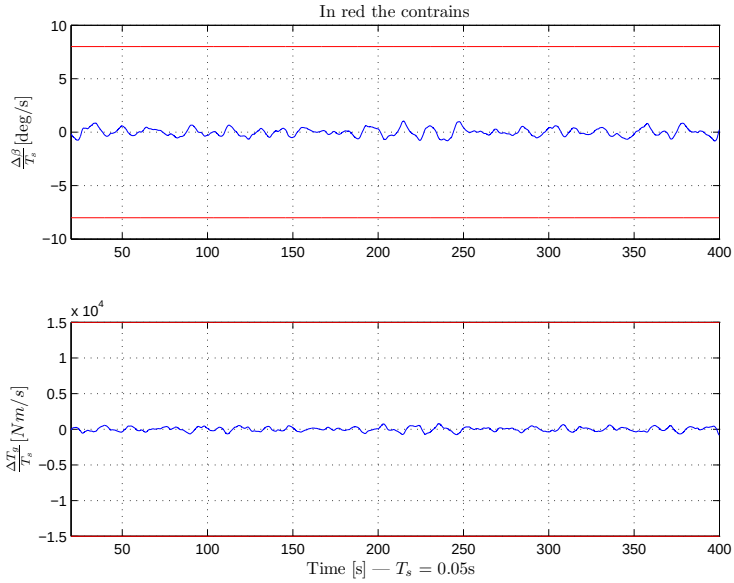

Figure 4.27: Pitch and torque derivative for baseline controller in region IV.

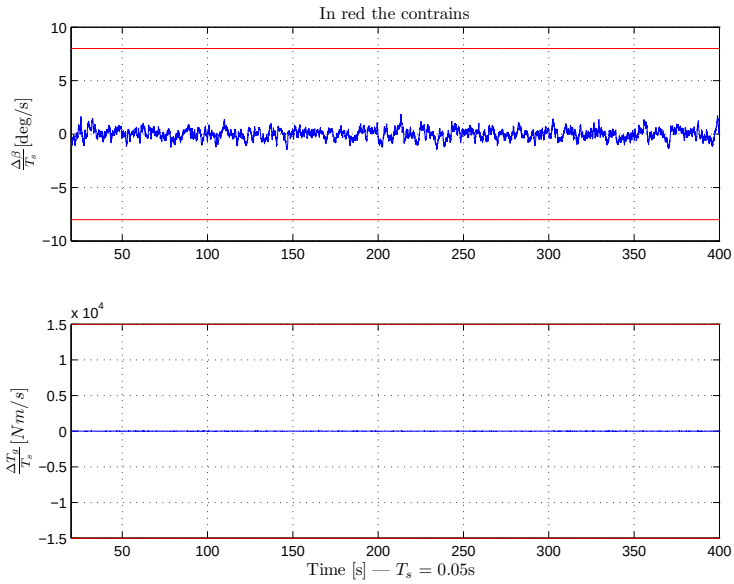

Figure 4.28: Pitch and torque derivative for LQG controller in region IV.

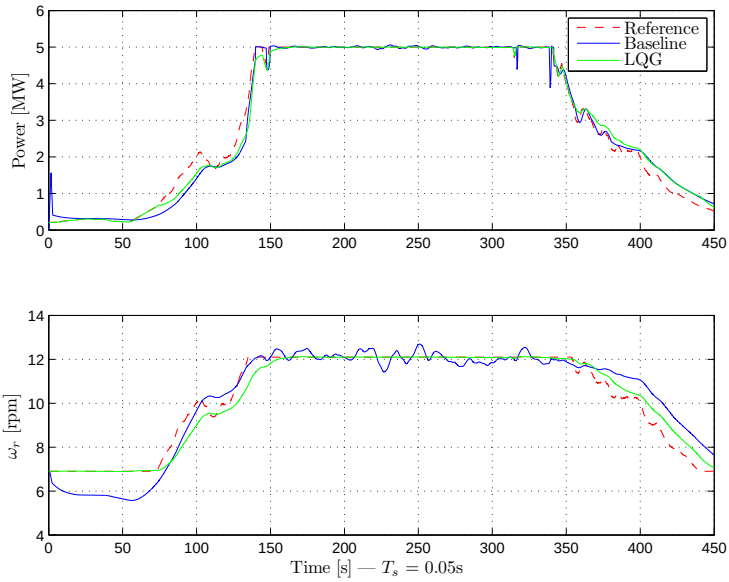

Figure 4.29: Electrical power and rotational speed comparison between baseline and LQG controller in all regions.

From this comparison one can conclude that the controller designed in this thesis is able to produce more electrical power than the baseline controller implemented by the *NREL*.

4.4.2 Stiff Vs. Hinge Tower

In this second comparison the control action is the same while the model used is different. On one case there is the WT0 with stiff tower while on the other case there is inverted pendulum turbine model with its hinge tower.

In figure 4.25 the stochastic wind introduced to make the comparison in region IV is shown. In figures 4.30 to 4.31 the results are shown.

From figure 4.30 it can be seen that with the hinge tower the variation on the electrical power and of the rotational speed is much bigger. The standard deviation in the electrical power for the inverted pendulum turbine is 24 times bigger than for the WT0 while for the rotational speed the standard deviation of the inverted pendulum turbine is 32 times bigger than for the WT0. From figure 4.31 one can see that with the hinge tower is much difficult to follow

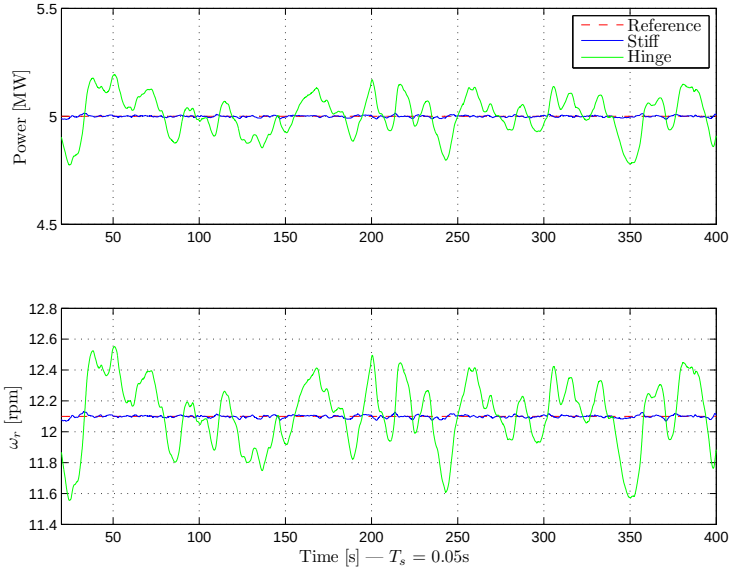

Figure 4.30: Electrical power and rotational speed comparison between stiff and hinge tower in region IV.

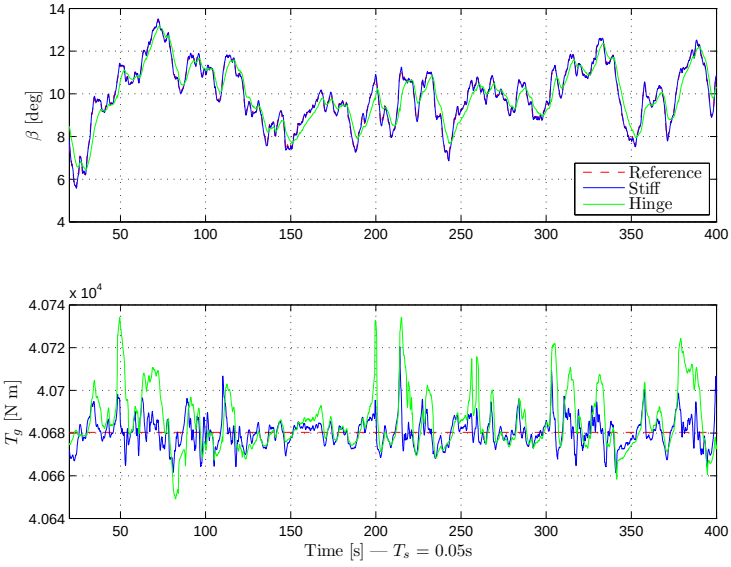

Figure 4.31: Pitch angle and generator torque comparison between stiff and hinge tower in region IV.

the pitch reference due to the fact that the controller in the inverted pendulum turbine has also the objective of keeping the tower in a certain inclination while in the WT0 model not.

In the inverted pendulum turbine the inclination of the tower needs to be kept in a certain angle. In the full load region, region IV, the pitch angle is trying to maximize the produced electrical power while keeping the tower in the appropriate inclination. This two objectives are difficult to achieve at the same time and as a result the produced electrical power has bigger variation.

Using as an input the stochastic wind defined in figure 4.20 one can obtain figures 4.32 and 4.33. With the data from 4.32 the electricity produced in 450 seconds for the inverted pendulum turbine is 372 kWh while for the WT0 is 384 kWh. In figure 4.33 it can be seen the pitch do not follow the reference in region II because the pitch actuator is busy keeping the tower in the appropriate inclination.

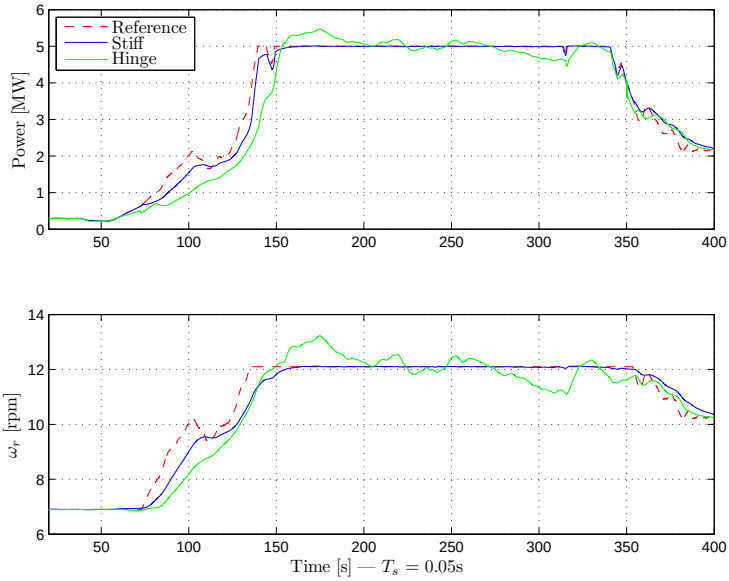

Figure 4.32: Electrical power and rotational speed comparison between stiff and hinge tower in all regions.

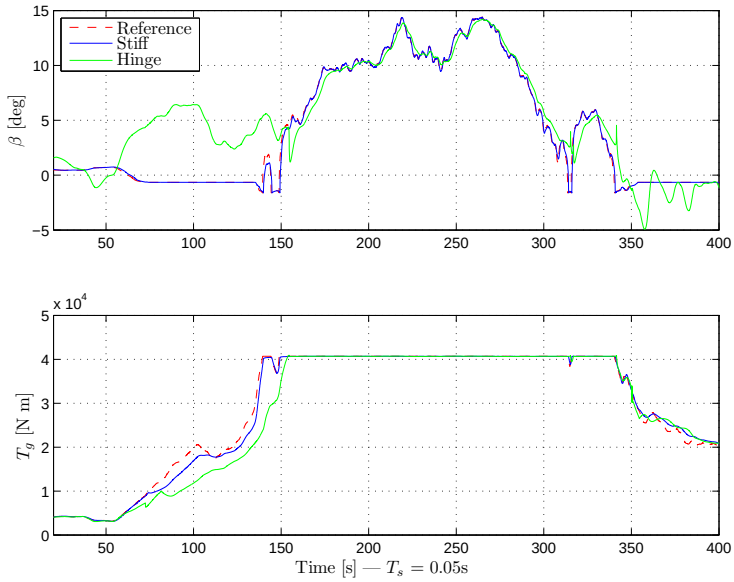

Figure 4.33: Pitch angle and generator torque comparison between stiff and hinge tower in all regions.

From this comparison one can conclude that trying to control the inverted pendulum turbine with the same control variables than a stiff tower turbine is difficult. As it was expected the electrical power produced with the inverted pendulum turbine is less than with a wind turbine with a stiff tower.

Chapter 5

Conclusions and Perspectives

In this chapter the conclusions of this project and the future perspectives of the inverted pendulum turbine are shown.

5.1 Conclusions

The main objective of this thesis is to study the feasibility of the inverted pendulum turbine. To reach this goal many sub-objectives have been achieved.

A model of the inverted pendulum turbine has been developed. The model considered is composed by a 2-order system of the hinge tower and a 1-order system of the rotor. The steady operation points for the inverted pendulum turbine have been obtained with the objective of maximizing the produced electrical power and keeping the hinge tower still. It has been shown that the steady state points of a stiff tower wind turbine and of a hinge tower wind turbine are the same but adding to the hinge tower the proper inclination angle. The non-linear model of the inverted pendulum turbine has been linearized at the steady operating points. The linear model obtained has been successfully compared with the non-linear one.

The model of the inverted pendulum turbine has been proved to be an unstable system, as it was expected. Using the same control inputs as current wind turbines, pitch angle β and generator torque T_g, it has been proved that the system is controllable. Having the measurements of the electrical power, the rotational speed and the angle of inclination is enough to be able to estimation of the states. All this measurements can easily be obtained with a proper sensor.

Once the model of the inverted pendulum turbine has been obtained and it has been proved that it can be controlled and observed the next step is designing the controller. It has been decided to use an optimal controller like the *Linear Quadratic Regulator*, which ensure a good performance, combined with an optimal estimator based on a *Kalman filter*. This technique is known as *Linear Quadratic Gaussian Control* and it has been introduced and used in this project. In order to get offset free control some methods like *Disturbance Modelling* and *Integral Action* have been studied.

The steady operation points of the inverted pendulum turbine define four different regions in the wind speed range, each one with different properties. In each region the controller designed has been tuned differently according to the control objective of the region. The region switching criteria used is based on the estimated wind. To get the wind estimation the inverted pendulum turbine model has been extended and a *Kalman filter* has been used. The final controller used in this project is a gain scheduling LQG controller based on the estimated wind.

Form the simulations it has been shown that the method used to estimate the wind is reliable. It has also been shown that the offset-free methods implemented do not provide such a good performance as it was expected. This could be explained for the undesirable effect of adding integrators to an unstable system. The controller implemented has been proved to have good performance in all the operation regions. It also has been shown that in the transition between regions III and IV there is an issue on keeping the pitch actuator constrains while trying to keep the tower in a proper inclination, this would need to be investigated.

The controller of the inverted pendulum turbine has been implemented on a stiff tower wind turbine and it has been compared with the baseline controller designed by the*NREL*. It has been shown that the regulator designed in this thesis is able to produce more electrical power than the designed by the *NREL*.

The performance of the inverted pendulum turbine has been compared with a stiff tower wind turbine regulated by the controller design in this thesis. It has been shown that the variation of the electrical power for the hinge turbine is higher than for the stiff tower turbine. This variation could be damped by the

wind park and at the point of connection with the grid the oscillations would be much lower. As it was expected the produced electrical power for the inverted pendulum turbine is lower than for the stiff tower wind turbine.

With all the things mentioned above now one can discuss the feasibility of the inverted pendulum turbine. It has been shown that the inverted pendulum turbine can be controlled with the pitch and the generator torque with the issue already mention in the transition III to IV which should be investigated. It has also been shown that from a control point of view the mass of the tower could be reduced having as a result a lighter and cheaper structure. From (Fingersh et al., 2006) the relation between the mass of the tower and its price is linear. Then from a control point of view the price of the tower could be reduced in a 20% having almost the same control problem, almost the same angle of inclination (4% bigger), while the produced electrical power would be slightly lower, according to figure 4.32 about 0.5% less. Then, from a control point of view and with deeper research on the issues mentioned, the inverted pendulum turbine is feasible. It is clear that the inverted pendulum turbine have new challenging problem to overcome, but the arising challenges from this design could be compensated by the benefit harvested.

5.2 Perspectives

This project is a first step on the investigation of the inverted pendulum turbine and it opens a wide range of possible future investigations and improvements.

On the modelling side of the project it would be very interesting to include additional effects and degrees of freedom to the model. Taking in account that the tower is moving forwards and backwards it would be interesting to model the relative wind speed over the rotor area. This consideration would lead to a stronger couple between the two sub-models implemented in this thesis: the rotor and the hinge turbine. Having a model which is able to evaluate the fatigue loads over the components of the wind turbine, for example the tower, would be really attractive from a mechanical point of view since the stress of the components could be analysed and minimized. Moreover, it would also be recommended to include the flexibility of the drive-train. This consideration leads to a dynamic angular displacement between the angle of the generator and the angle of the rotor. Adding models of the pitch and the torque actuators would make the model of the inverted pendulum wind turbine more realistic. Besides all this improvements, it would be very interesting to include the effect of the yaw angle and the angle of inclination of the wind turbine, omitted in this project, with all the mechanical consequences derived from that.

Regarding the control part of the project there are some future implementations that would be very interesting to develop. First of all designing a controller which objectives, besides maximizing produced electrical power and keeping the tower still, would be minimizing the stress of the components. That would be a very interesting approach since as a consequence the cost of this components could be reduced. The regulator designed in this thesis is able to control the inverted pendulum turbine when it is running but non start-up and stop techniques have been implemented. This techniques should be investigated to bring the inverted pendulum turbine from a safety looked position to a running one and vice versa. Researching in this methods is crucial for a possible future application of this uncommon wind turbine. Another interesting research would be to study the possible existence of harmonic disturbances introduced in the electrical power by the controller.

The control problem solved in this thesis can be extrapolated in the offshore case. The hinge effect in the offshore case could be achieved with a floating foundation controlled by some kind of mechanical actuator. This approach would allow to place offshore wind farms in deep waters, where the quality of the wind is better for power extraction. As the reader can see the inverted pendulum turbine open a wide range of possibilities that in a close future could improve the wind energy world and as a direct consequence the world energy system.

Appendix A

Tower Spring-Mass-Damper Justification

The tower of a wind turbine can be modelled as a spring-mass-damper system not effected by the gravity as shows A.1.

$$F_t = M_t\ddot{x}_t + D_t\dot{x}_t + K_t x_t \tag{A.1}$$

Since the data from this constants were not provided in the reference document the constants of this model have been determined with data available in (Jonkman et al., 2009) as shown below

$$M_t = m_{tower} + m_{nancelle} + m_{rotor} + m_{hub} \tag{A.2}$$

$$K_t = (f_n 2\pi)^2 Mt \tag{A.3}$$

$$D_t = 0.01K_t \tag{A.4}$$

The equation A.3 comes from basics physics, where f_n is the natural frequency in Hz. The equation A.4 is a rule of thumb.

Since this project is working in angle of inclination instead of displacement all the constants have been changed accordingly.

Appendix B

System Parameters

In this appendix all the data used in the simulations is displayed. There are two consideration to be made about table B.2:

- The total inertia of the generator and the rotor, J, is expressed with respect to the low shaft.
- The spring K_t and damping constants D_t of the tower are the ones obtained in the appendix A.

Table B.1: Physical Constants.

Parameter	**Symbol used**	**Value**	**Units**
Air density	ρ_a	1.2041	kg/m^3
Gravity	g	9.81	m/s^2

Table B.2: Baseline Wind Turbine Characteristics. (Jonkman et al., 2009)

Parameter	**Symbol**	**Value**	**Units**
Rated power	P_{rated}	5	MW
Cut-in wind speed	v_{cut-in}	3	m/s
Cut-out wind speed	$v_{cut-out}$	25	m/s
Cut-in rotor speed	$\omega_{r_{min}}$	6.9	rpm
Rated rotor speed	$\omega_{r_{rated}}$	12.1	rpm
Rotor radius	R	63	m
Hub heigh	h_1	90	m
Tower center of mass heigh	h_2	38.234	m
Rotor mass	m_{rotor}	110.000	kg
Nacelle mass	$m_{nacelle}$	240.000	kg
Hub mass	m_{hub}	56.780	kg
Tower mass	m_2	347.460	kg
Top mass(rotor, nacelle and hub)	m_1	406.780	kg
Gear box ratio	N	97:1	-
Inertia of the generator	J_g	534.116	$kg\ m^2$
Inertia of the rotor	J_r	3.8768e7	$kg\ m^2$
Inertia of the generator and rotor	J	4.3792e7	$kg\ m^2$
Spring constant of the tower	K_t	3.1296e6	N/m
Damping constant of the tower	D_t	31.296	N/ms
Total mass (tower,rotor, nacelle and hub)	M_t	754.240	kg
Natural frequency of the tower Fore-Aft	f_n	0.3240	Hz
Maximum generator torque speed	$\dot{T}_g$	15.000	N m
Maximum generator torque	$T_{g,max}$	47.402.91	N m
Maximum pitch speed	$\dot{\beta}$	8	deg/s
Maximum pitch rate	$T_{g,max}$	90	deg

Bibliography

Burton, T., Shrape, D., Jenkins, N., and Bossanyi, E. (2001). *Wind Energy Handbook*. John Wiley.

Fingersh, L., Hand, M., and Laxson, A. (2006). Wind Turbine Design Cost and Scaling Model. Technical report, National Renewable Energy Laboratory, U.S.

Franklin, G., Powel, J., and Emami-Naeini, A. (2002). *Feedback Control of Dynamic Systems*. Prentice-Hall.

Friis, J., Nielsen, E., and Bonding, J. (2010). Repetitive Individual Pitch Model Predictive Control for Horitzontal Axis Wind Turbine. Master's thesis, Aalborg University.

Gosk, A. (2011). Model Predictive Control of a Wind Turbine. Master's thesis, Technical University of Denmark.

Hammerum, K. (2006). A Fatigue Approach to Wind Turbine Control. Master's thesis, Technical University of Denmark.

Hansen, M. (2008). *Aerodynamics of Wind Turbines*. Earthscan.

Hendricks, E., Jannerup, O., and Sørensen, P. (2008). *Linear Systems Control: Deterministic and Stochastic Methods*. Springer.

Henriksen, L. C. (2007). Model Predictive Control of a Wind Turbine. Master's thesis, Technical University of Denmark.

Jonkman, J., Butterfield, S., Musial, W., and Scott, G. (2009). Definition of a 5-MW Reference Wind Turbine for Offshore System Development. Technical report, National Renewable Energy Laboratory, U.S.

Kedjar, B. and Al-Haddad, K. (2009). DSP-Based Implementation of an LQR with Integral Action for a Three-Phase Three-Wire Shunt Active Power Filter. *IEEE Transaction on Industrial Electronics*, 56(8).

Madsen, M. and Filsø, J. (2012). Preview-Based Asymmetric Load Reduction of Wind Turbines. Master's thesis, Aalborg University.

Mirzaei, M., Henriksen, L. C., Poulsen, N. K., Niemann, H. H., and Hansen, M. H. (2012a). Individual Pitch Control Using LIDAR Measurements. In *IEEE Multi-Conference on Systems and Control*, Dubrovnik, Croatia.

Mirzaei, M., Poulsen, N. K., and Niemann, H. H. (2012b). Robust Model Predictive Control of a Wind Turbine. In *American Control Conference*, Montreal, Canada.

Muske, K. and Badgwell, T. (2002). Disturbance Modeling for Offset-Free Linear Model Predictive Control. *Journal of Process Control*, 12(5).

Østergaard, K., Brath, P., and Stoustrup, J. (2007). Estimation of Effective Wind Speed. *Journal of Physics: Conference Series 75*.

Pannocchia, G. and Rawlings, J. (2003). Disturbance Models for Offset-Free Model-Predictive Control. *AIChE Journal*, 49(2).

Poulsen, N. K. (2012a). Set Point Control in the State Space Setting.

Poulsen, N. K. (2012b). Stochastic Adaptive Control. Lecture Notes, `http://www2.imm.dtu.dk/courses/02421/tfoils.pdf`.

Proakis, J. and Manolakis, D. (2007). *Digital Signal Processing*. Pearson Prentice Hall.

Sathyajith, M. (2006). *Wind Energy: Fundamentals, Resource Analysis and Economics*. Springer-Verlag Berlin Heidelberg.

Skogestad, S. and Postlethwaite, I. (2005). *Multivariable Feedback Control: Analysis and Design*. John Wiley.

Slotine, J. and Li, W. (1991). *Applied Nonlinear Control*. Prentice-Hall.

Xin, M., Poulsen, N., and Bindner, H. (1997). Estimation of the Wind Speed in Connection to Wind Turbines. In *Proceedings of the IASTED Internation Conference CONTROL'97*, Mexico, Cancun.